As you are now the owner of this document which should have come to you for free, please consider making a donation of £1 or more for the upkeep of the (Radar) website which holds this document. I give my time for free, but it costs me in excess of £300 a year to bring these documents to you. You can donate here https://blunham.com/Radar

Please do not upload this copyright pdf document to any other website. Breach of copyright may result in a criminal conviction.

This document was generated by me Colin Hinson from a document held at Henlow Signals Museum. It is presented here (for free) and this version of the document is my copyright (along with the Signals Museum) in much the same way as a photograph would be. Be aware that breach of copyright can result in a criminal record.

The document should have been downloaded from my website https://blunham.com/Radar, if you downloaded it from elsewhere, please let me know (particularly if you were charged for it). You can contact me via my Genuki email page: https://www.genuki.org.uk/big/eng/YKS/various?recipient=colin

You may not copy the file for onward transmission of the data nor attempt to make monetary gain by the use of these files. If you want someone else to have a copy of the file, please point them at the website (https://blunham.com/Radar).

Please do not point them at the file itself as the file may move or be updated.

I put a lot of time into producing these files which is why you are met with this page when you open the file.

In order to generate this file, I need to scan the pages, split the double pages and remove any edge marks such as punch holes, clean up the pages, set the relevant pages to be all the same size and alignment. I then run Omnipage (OCR) to generate the searchable text and then generate the pdf file.

Hopefully after all that, I end up with a presentable file. If you find missing pages, pages in the wrong order, anything else wrong with the file or simply want to make a comment, please drop me a line (see above).

It is my hope that you find the file of use to you personally – I know that I would have liked to have found some of these files years ago – they would have saved me a lot of time !

Colin Hinson
In the village of Blunham, Bedfordshire.

RRE journal

R.R.E.

OCTOBER 1955

R. R. E. J O U R N A L

CONTENTS

Issued by the Radar Research Establishment, Ministry of Supply

No. 37 October 1955

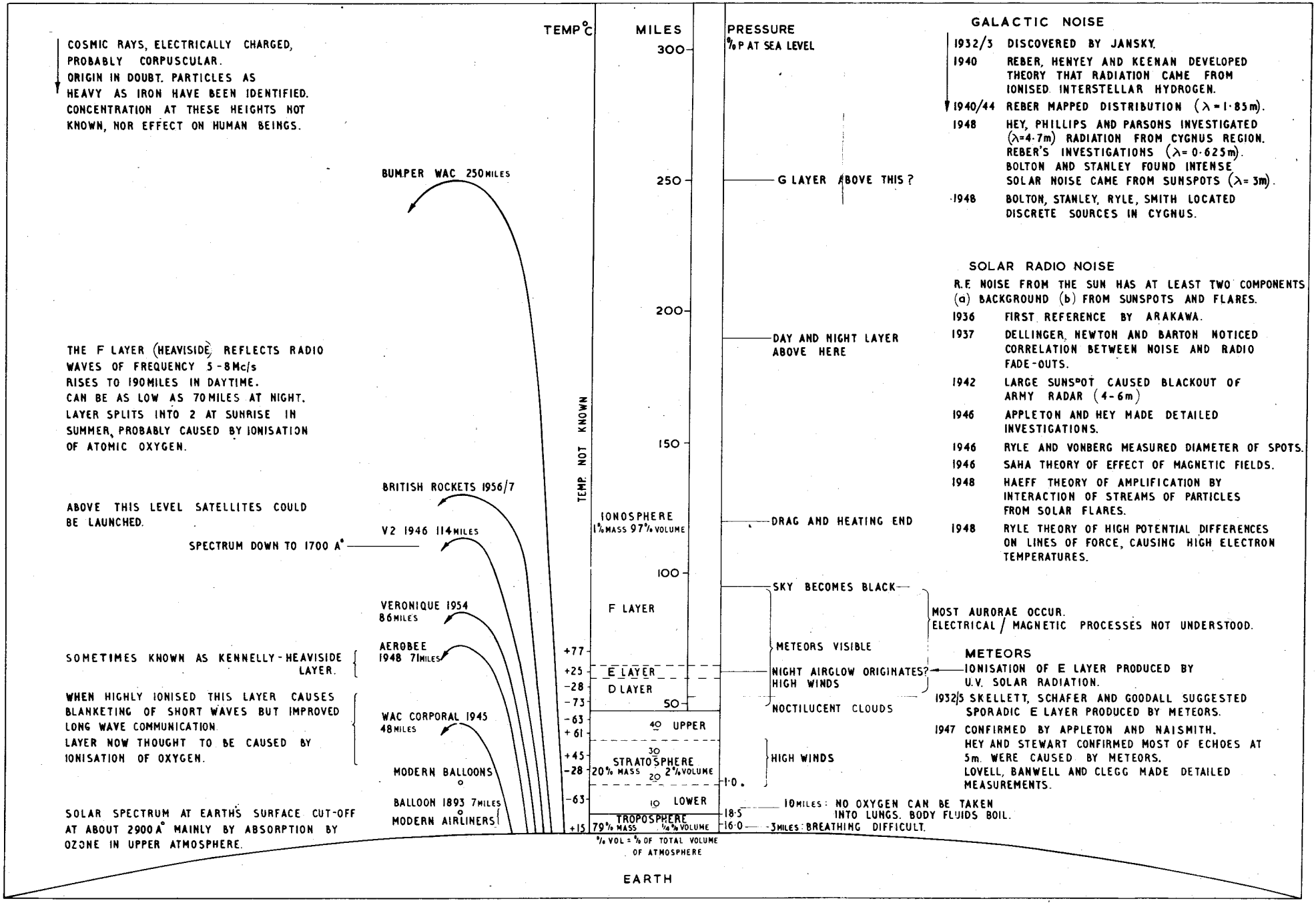
COSMIC RAYS, ELECTRICALLY CHARGED, PROBABLY CORPUSCULAR. ORIGIN IN DOUBT. PARTICLES AS HEAVY AS IRON HAVE BEEN IDENTIFIED. CONCENTRATION AT THESE HEIGHTS NOT KNOWN, NOR EFFECT ON HUMAN BEINGS.
TEMP °C
MILES
PRESSURE % P AT SEA LEVEL
300
250
200
150
100
50
BUMPER WAC 250 MILES
G LAYER ABOVE THIS ?
DAY AND NIGHT LAYER ABOVE HERE
DRAG AND HEATING END
SKY BECOMES BLACK
METEORS VISIBLE
NIGHT AIRGLOW ORIGINATES? HIGH WINDS
NOCTILUCENT CLOUDS
HIGH WINDS
10 MILES: NO OXYGEN CAN BE TAKEN INTO LUNGS. BODY FLUIDS BOIL.
3 MILES: BREATHING DIFFICULT.
TEMP. NOT KNOWN
IONOSPHERE 1% MASS 97% VOLUME
F LAYER
E LAYER
D LAYER
40 UPPER
30
STRATOSPHERE 20% MASS 20 2% VOLUME
10 LOWER
TROPOSPHERE 79% MASS 1/4% VOLUME
+77
+25
-28
-73
-63
+61
+45
-28
-63
+15
1·0
18·5
16·0
% VOL = % OF TOTAL VOLUME OF ATMOSPHERE
EARTH
THE F LAYER (HEAVISIDE) REFLECTS RADIO WAVES OF FREQUENCY 5 - 8 Mc/s RISES TO 190 MILES IN DAYTIME. CAN BE AS LOW AS 70 MILES AT NIGHT. LAYER SPLITS INTO 2 AT SUNRISE IN SUMMER, PROBABLY CAUSED BY IONISATION OF ATOMIC OXYGEN.
ABOVE THIS LEVEL SATELLITES COULD BE LAUNCHED.
BRITISH ROCKETS 1956/7
V2 1946 114 MILES
SPECTRUM DOWN TO 1700 A°
VERONIQUE 1954 86 MILES
AEROBEE 1948 71 MILES
SOMETIMES KNOWN AS KENNELLY - HEAVISIDE LAYER.
WHEN HIGHLY IONISED THIS LAYER CAUSES BLANKETING OF SHORT WAVES BUT IMPROVED LONG WAVE COMMUNICATION. LAYER NOW THOUGHT TO BE CAUSED BY IONISATION OF OXYGEN.
WAC CORPORAL 1945 48 MILES
MODERN BALLOONS
BALLOON 1893 7 MILES
MODERN AIRLINERS
SOLAR SPECTRUM AT EARTHS SURFACE CUT-OFF AT ABOUT 2900 A° MAINLY BY ABSORPTION BY OZONE IN UPPER ATMOSPHERE.
GALACTIC NOISE
1932/3 DISCOVERED BY JANSKY.
1940 REBER, HENYEY AND KEENAN DEVELOPED THEORY THAT RADIATION CAME FROM IONISED INTERSTELLAR HYDROGEN.
1940/44 REBER MAPPED DISTRIBUTION (λ = 1·85m).
1948 HEY, PHILLIPS AND PARSONS INVESTIGATED (λ=4·7m) RADIATION FROM CYGNUS REGION. REBER'S INVESTIGATIONS (λ= 0·625m). BOLTON AND STANLEY FOUND INTENSE SOLAR NOISE CAME FROM SUNSPOTS (λ= 3m).
1948 BOLTON, STANLEY, RYLE, SMITH LOCATED DISCRETE SOURCES IN CYGNUS.
SOLAR RADIO NOISE
R.F. NOISE FROM THE SUN HAS AT LEAST TWO COMPONENTS (a) BACKGROUND (b) FROM SUNSPOTS AND FLARES.
1936 FIRST REFERENCE BY ARAKAWA.
1937 DELLINGER, NEWTON AND BARTON NOTICED CORRELATION BETWEEN NOISE AND RADIO FADE-OUTS.
1942 LARGE SUNSPOT CAUSED BLACKOUT OF ARMY RADAR (4-6m)
1946 APPLETON AND HEY MADE DETAILED INVESTIGATIONS.
1946 RYLE AND VONBERG MEASURED DIAMETER OF SPOTS.
1946 SAHA THEORY OF EFFECT OF MAGNETIC FIELDS.
1948 HAEFF THEORY OF AMPLIFICATION BY INTERACTION OF STREAMS OF PARTICLES FROM SOLAR FLARES.
1948 RYLE THEORY OF HIGH POTENTIAL DIFFERENCES ON LINES OF FORCE, CAUSING HIGH ELECTRON TEMPERATURES.
MOST AURORAE OCCUR. ELECTRICAL / MAGNETIC PROCESSES NOT UNDERSTOOD.
METEORS
IONISATION OF E LAYER PRODUCED BY U.V. SOLAR RADIATION.
1932/5 SKELLETT, SCHAFER AND GOODALL SUGGESTED SPORADIC E LAYER PRODUCED BY METEORS.
1947 CONFIRMED BY APPLETON AND NAISMITH. HEY AND STEWART CONFIRMED MOST OF ECHOES AT 5m. WERE CAUSED BY METEORS. LOVELL, BANWELL AND CLEGG MADE DETAILED MEASUREMENTS.

THE DESIGN OF A VERY-LOW-NOISE 800 c/s SELECTIVE AMPLIFIER AND INPUT TRANSFORMERS

By P. J. Baxandall, B.Sc. (Eng.)

1. INTRODUCTION AND GENERAL DESCRIPTION

The apparatus described in this paper was designed* to satisfy a need for an audio-frequency amplifier of sufficiently good noise factor to enable measurements to be made of the noise output from fractional-ohm resistors and signal sources, operating at temperatures in the region of 20°K. The main requirement was to obtain a satisfactory performance at frequencies close to 800 c/s, the amplifier incorporating a selective circuit tuned to this frequency, but an additional, alternative, requirement was that the equipment should have a broadband response extending over four octaves centred on 800 c/s, i.e. from 200 c/s to 3200 c/s, with not more than 3 dB drop in gain at these extreme frequencies.

The low temperatures are obtained by placing the source at the bottom of a suitable cryostat, and very thin connecting leads must be used in order to avoid too high a rate of heat conduction down them. The amount of Johnson noise generated in the warmer parts of such leads would swamp that produced in the source if the leads were connected directly to the source, and it is therefore necessary to have an impedance step-up transformer situated in the low-temperature section of the cryostat. It has been found that a mumetal-cored transformer of normal construction will operate satisfactorily at temperatures at least as low as 14°K, though, as described in Section 2.1, allowance must be made, in designing the transformer, for the reduced permeability obtained at such temperatures.

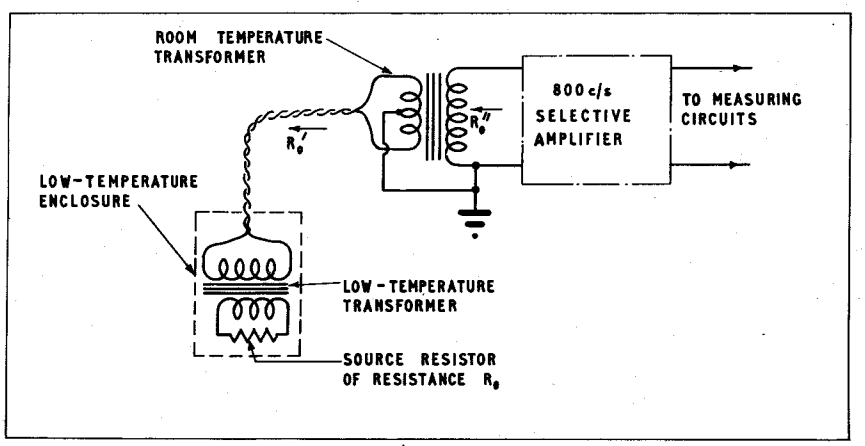

Figure 1

Block Schematic Diagram of System Used

The complete system is shown in Figure 1, from which it will be seen that two transformers are used in cascade. The "low-temperature" transformer steps up the source impedance to approximately 300 ohms, which is an impedance level suitable to allow the use of a number of feet of twisted and screened balanced line between this transformer and the "room-temperature" transformer in the amplifier chassis. To make valve noise as small as possible relative to the noise from the source, the room-temperature transformer should step up to the highest practicable secondary impedance; a value of 1 megohm is adopted in the equipment here described.

It would have been possible, of course, to have employed only one transformer, operating at low temperature and stepping up directly to a very high impedance; but considerable advantages result from doing the impedance transformation in two stages, for the following reasons:-

(a) The low-temperature transformer must be physically very small, in order to allow it to be accommodated in the cryostat, which would make it very difficult to wind the large number of turns (at least 20,000) that would be required on the secondary for stepping directly up to grid impedance. The number of turns required for stepping up to 300 ohms is, however, only about 1000, and the transformer is then very easy to wind - several transformers can be readily made, if required, to suit sources of different internal resistances.

(b) The necessity of keeping the stray capacity on the high-impedance secondary very low would make it essential, with the single-transformer system, to have the amplifier very close to the cryostat and, even if this were carefully arranged, it is almost inevitable that the total stray capacity would be higher than with a separate transformer close to the input-valve grid. By using two transformers, the amplifier may be placed on the bench at a convenient distance from the cryostat, well away from the stray field and vibration of vacuum pump motors, etc.

The disadvantage of employing a separate high-impedance transformer in the amplifier chassis is that all loss resistances associated with this transformer, being at room temperature, contribute much more Johnson noise than the same values of resistance would do if at low temperature. The main causes of the loss resistances concerned are:-

(a) Copper resistance, appearing in series with each winding.

(b) Resistance of eddy current paths in the core - best represented by an equivalent resistance in shunt with one of the windings.

(c) Insulation losses, which can also be represented as in (b).

It should be noted that hysteresis losses are always quite negligible in a very low level transformer, and therefore do not need to be considered in the present problem.

Each resistance in the system will have an effective Johnson noise voltage acting in series with it, given by:-

$$V_N = \sqrt{4kTR\delta f} \qquad \ldots (1)$$

where V_N = r.m.s. noise voltage in volts.
k = Boltzmann's Constant = 1.380×10^{-23} Joules/°C.
T = Absolute temperature of resistance in °K.
R = Resistance in ohms.
δf = Effective bandwidth in c/s over which noise is measured.

The problem in designing the transformers is to ensure that the total noise contributed by all resistances other than the source itself is adequately small in relation to the source noise.

In Appendix 1 it is shown that, to make the noise contribution due to any shunt resistance negligible, the shunt resistance must be high compared with the impedance of the circuit across which it appears, particularly when the shunt resistance is at a higher temperature than that of the source. Thus, for example, an eddy-current shunt resistance of 15 megohms, appearing across the secondary of the room-temperature transformer, assuming the source resistance to have been stepped up to 1 megohm, would contribute an amount of Johnson noise approximately equal to that coming from the source if the source temperature were 20°K and the room temperature were 300°K. An eddy-current shunt resistance several times greater than 15 megohms was therefore aimed at in the present equipment.

In addition to the requirement for high values of shunt resistance, any series resistance must be correspondingly small in relation to the impedance of the circuit in series with which it appears, and it is consequently necessary, in designing the room-temperature transformer, to make the ratio of the shunt loss resistance to the series loss resistance much higher than is required in a normal low-level audio-frequency input transformer. The considerations which are involved in achieving this aim are discussed in detail in Section 3, but it may be noted at this stage that a satisfactory performance has been obtained by a combination of the following features:-

(a) A large size of core
(b) Thin mumetal laminations
(c) Carefully-chosen numbers of turns on the windings.

The low-temperature and room-temperature transformers are shown in Figures 2(a) and 2(b) respectively, a tall and narrow secondary winding being adopted in the room-temperature transformer in order to keep the secondary stray capacity down to less than 50 pF and thus to allow a very high secondary impedance to be used.

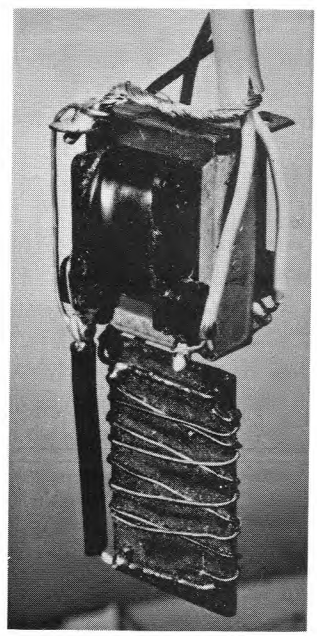

Figure 2(a)
Low-Temperature Transformer

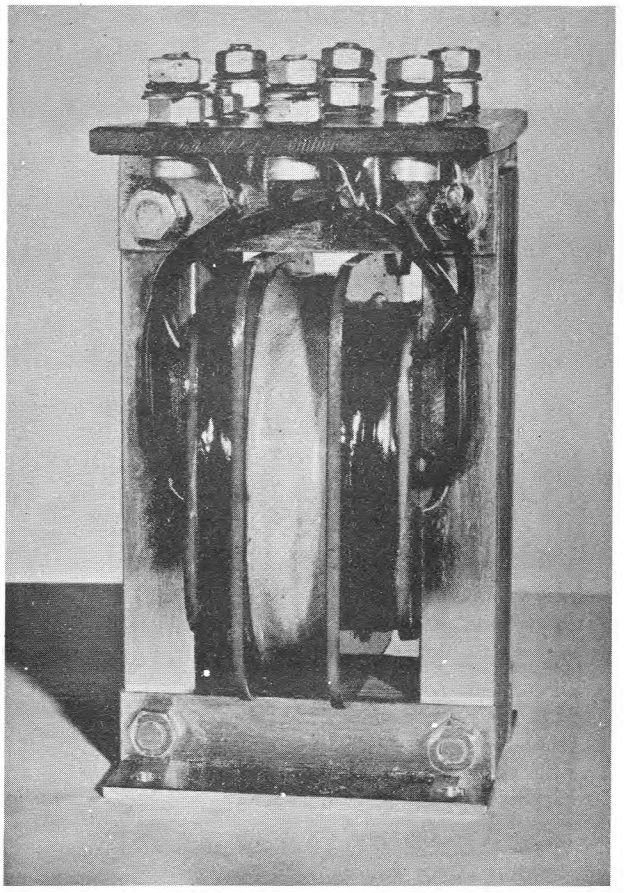

Figure 2(b)
Room-Temperature Transformer

The amplifier circuit (Figure 3) employs three pentodes, and has a total H.T. consumption of less than 5 mA at 300 V. Negative feedback, mainly to improve the gain-stability, is applied by means of a resistive network between the cathodes of the first and last valves. The tuned circuit is in the anode lead of the last valve, and is therefore outside the feedback loop; but the feedback results in the effective output impedance of the amplifier, as seen by the tuned circuit, being very high and therefore such as to introduce very little extra damping. The tuned circuit may be replaced by a resistance when required, giving a broad-band frequency response, with both transformers in use, extending from 200 c/s to 3200 c/s with less than 3 dB fall-off.

The feedback network may be switched to give gain values, between the input grid and the output valve anode at 800 c/s, of 10^2, 10^3, 10^4 and 10^5. The low-gain settings are intended for use in experiments other than noise measurements, but it is an advantage of achieving the gain reduction by means of feedback that the amplifier is able to handle large signal inputs with low distortion whilst still retaining the same

good noise factor [1] as at the highest-gain setting. In order to limit the loop gain at the low overall gain settings of the switch, local feedback round the middle stage is also varied by the same control. The amount of overall feedback at working frequencies varies from approximately 36 dB on the $x10^2$ range to approximately 20 dB on the $x10^5$ range.

Care had to be taken over the choice of the input valve and its operating conditions, to ensure that the total valve noise should be adequately low. The main causes of valve noise[2] are:-

(a) Shot noise
(b) Partition noise (if a pentode)
(c) Grid-current noise
(d) Flicker noise

An effect known as "induced grid noise"[2] was considered but found to be quite negligible at audio frequencies. In addition to making the above sources of noise adequately small, it is very important to take suitable precautions to minimise microphony, interference pick-up and hum [3].

At the time the amplifier was designed, it was believed that a significant contribution would probably arise from flicker noise, but some experiments done more recently, together with the results of some unpublished work by G. R. Nicoll of R.R.E., have led to the belief that, with a good sample of input valve, flicker noise is normally negligible at 800 c/s when working at anode currents of 1 mA or less. This point is discussed in greater detail in Section 5.

A pentode input valve was chosen mainly because of the high stage gain obtainable, the noise contribution due to partition effect being small enough, in relation to the other contributions in the system, to be unimportant in practice.

Grid-current noise arises from the fact that grid current, like anode current, has shot-noise fluctuations superimposed on it; these fluctuations, flowing in the grid-circuit impedance, give rise to small fluctuations in grid voltage and thus contribute to the noise output from the amplifier. It is thus evident that grid-current noise will be most noticeable when the grid-circuit impedance is very high, particularly when, as in the present instance, the effective temperature of the grid-circuit impedance is low and its Johnson noise therefore abnormally low.

Noise due to grid current is considered in greater detail in Section 6, but it may be mentioned here that if the grid current in the apparatus described in this paper had been allowed to be as high as 10^{-8} A, grid-current noise would have been by far the largest contribution in determining the noise factor of the system.

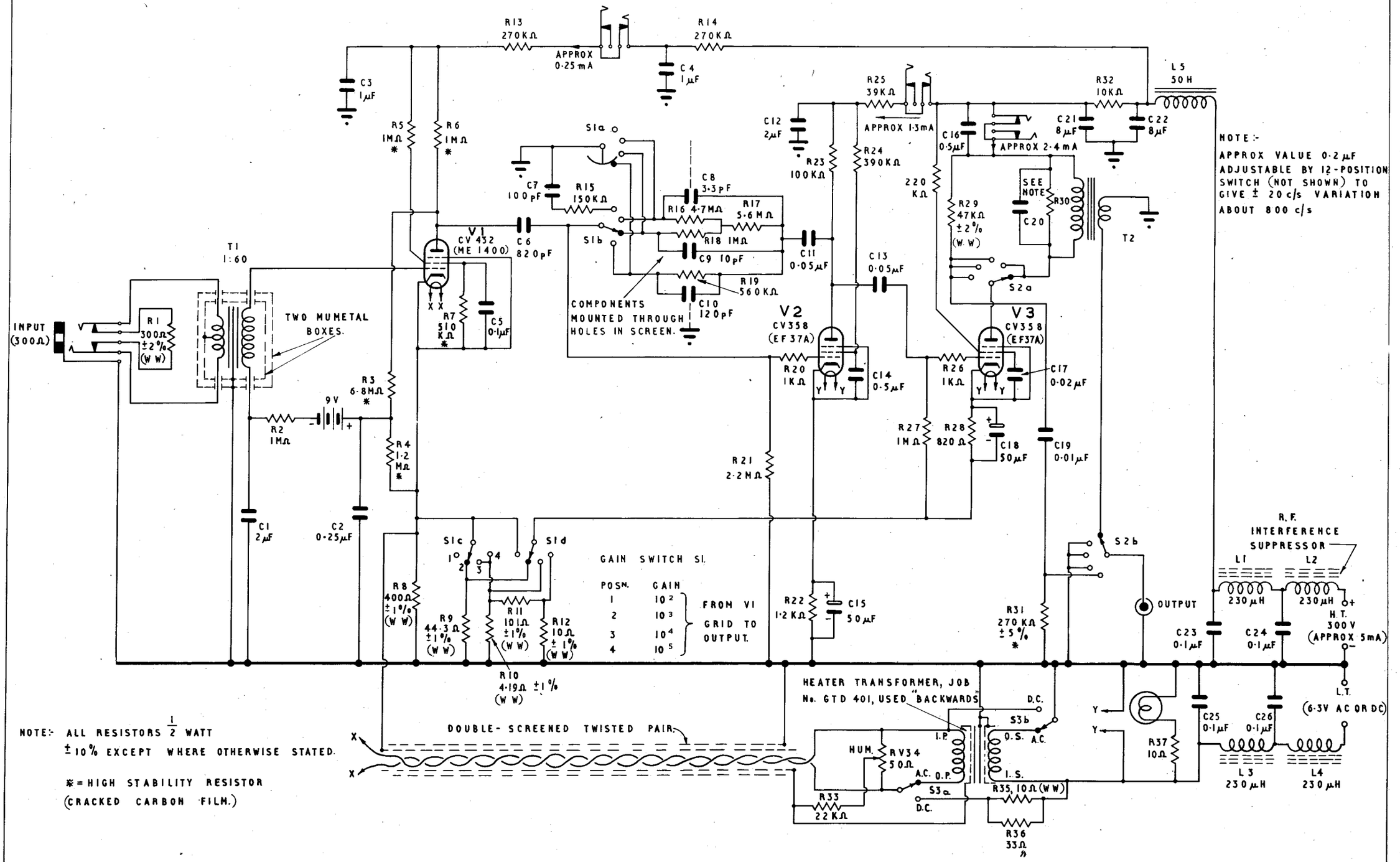

FIG. 3.
LOW-NOISE 800 c/s. AMPLIFIER.

When the equipment was designed, the manner in which the grid current of a valve would vary with the operating conditions was not clearly appreciated, and it was therefore decided to play for safety by using an ME1400 valve* operating approximately under the conditions which were stated by the makers to give a grid current not greater than 10^{-11} A, a value low enough to ensure that grid-current noise would be negligible in relation to other contributions. The recommended conditions are $V_a = V_{g2} = 45$ V, $(I_a + I_{g2}) = 150$ μA, $V_{htr} = 4.5$V; the required negative control grid bias is then about 2V, which is sufficient to ensure that only a neglibible fraction of the grid current is due to the collection of electrons by the grid.

Under the operating conditions mentioned in the previous paragraph, the only significant valve noise contributions in the equipment are shot noise and partition noise, which may be represented by an equivalent room-temperature resistance in series with the grid of an ideal noiseless valve. It is then evident that, provided grid-current noise remains negligible, the higher the grid-circuit impedance to which the source is stepped up, the less significant will the valve noise become in relation to that from the source.

It is possible to calculate (see Appendix 2) the magnitude of all the individual noise contributions in the transformers and in the amplifier, and thus to arrive at a theoretical noise factor for the complete system for any specified source temperature. Curve (a) in

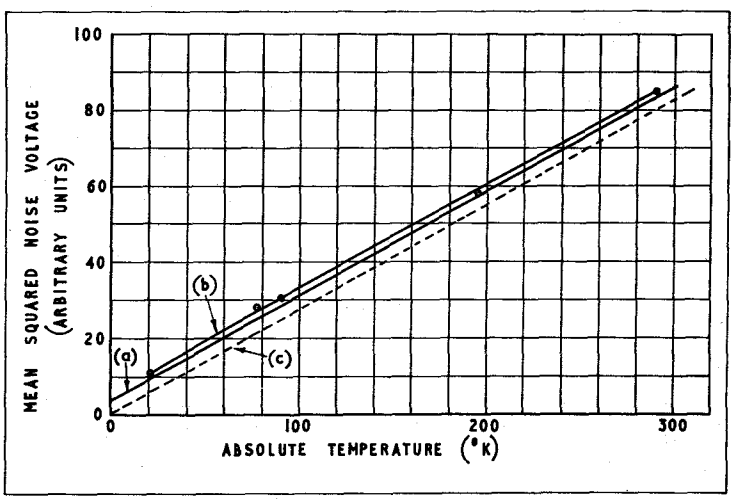

Figure 4

Variation of Mean Squared Noise Voltage with Absolute Temperature

Curve (a) - Initial calculated curve
Curve (b) - Experimental curve
Curve (c) - Ideal curve

*The ME1400 (CV432, VX8048) is a selected and aged version of the Mullard EF37A, selected for low grid current.

Figure 4 shows how the calculated mean square noise output from the amplifier would be expected to vary with the temperature of the source. Curve (b) shows the corresponding result obtained experimentally; the difference between the two curves is mainly due to the fact that the measured shunt loss resistance of the room-temperature transformer shown in Figure 2(b), which was the transformer in use when curve (b) was obtained, was only about half the calculated value. As explained in Section 3, the reason for the unexpectedly low shunt loss resistance was later found to be dielectric losses in the paxolin coil former used in the transformer of Figure 2(b). A second transformer was built, with a polystyrene coil former, and gave the predicted value of shunt loss resistance. An opportunity for obtaining an experimental curve corresponding to curve (b) but with the improved transformer design in use has not presented itself, but it can be predicted with confidence that the curve would almost coincide with curve (a). The noise factor for curve (b), with the source at 20°K, is 2.7 dB. It will be noticed that the experimental curve of Figure 4 was obtained with a 300 ohm wirewound resistor feeding directly to the room-temperature transformer. At temperatures in the region of 20°K, a result indistinguishable from that shown was obtained when the 300 ohm resistor was replaced by the 0.45 ohm resistor and small transformer shown in Figure 2(a), but, with the latter arrangement, somewhat more noise was obtained at higher temperatures; this was just as expected, however, since the winding resistances of the small transformer, though quite negligible at 20°K, become appreciable at higher temperatures and therefore contribute a significant amount of noise.

It may be worth mentioning that when the first experiments were performed after building the equipment, a noise factor in the region of 6 dB was obtained when the source was at 20°K, the exact value varying somewhat from one determination to another. After investigating various possible causes of this unexpectedly high value, it was ultimately found to be due to microphony of the room-temperature transformer, which was being excited by sounds from machines in a generator room not far from the laboratory! This trouble was readily cured by adopting suitable anti-microphonic mounting arrangements for the transformer and input valve (see Section (4)).

The performance indicated by curve (b) of Figure 4 was regarded as quite adequate for the primary purpose for which the apparatus was built, and much successful work has in fact been done with its aid. Since designing the equipment, however, some effort has been devoted to investigating, in greater detail, the factors which set the ultimate limit to the reduction of noise level that can be achieved in amplifiers of the present type. The investigation was undertaken largely because the following considerations made it seem uncertain whether, in order to make the total valve noise as small as possible in relation to the source noise, it was in fact correct

to step up to the highest possible impedance at the input valve grid:-

(a) Provided grid-current noise is negligible in relation to shot and partition noise, it is evident that the higher the source resistance referred to the valve grid - denoted by R_o'' - the less will be the valve noise in relation to the source noise, since the valve noise can then be represented by an equivalent room-temperature resistance of fixed value in series with the grid.

(b) If, keeping the valve operating conditions the same, one continues to raise the effective source resistance R_o'', the source noise voltage at the grid will be proportional to $(R_o'')^{\frac{1}{2}}$, whereas the grid-current noise voltage at the grid will be proportional to R_o''. Consequently the grid-current noise must ultimately override the source noise if R_o'' is made sufficiently large. If, on the other hand, R_o'' is made sufficiently small, the shot noise will override the source noise; there must, therefore, be an optimum value of R_o'' for the total valve noise to be as small as possible relative to the source noise.

(c) The optimum value of R_o'' will depend on the current and voltage at which the input valve is run, low-current low-voltage operation giving low grid current but a high value of equivalent shot and partition noise resistance, and vice versa[2]. With low-current low-voltage operation, the optimum value of R_o'' becomes very high, but the equivalent shot and partition noise resistance is also high. Unless a good deal is known about the way in which grid current and equivalent noise resistance vary with operating conditions, it is not possible to say whether the optimum noise factor for low current and voltage operation will be better or worse than the optimum noise factor obtainable with the valve running at higher current and voltage.

The results of the investigation are given in detail in Section 5. The general conclusion is that, even when grid-current noise is fully taken into account, it still pays to step up to the highest practicable grid impedance, the valve operating conditions being adjusted, if possible, to make the sum of the shot and partition noise approximately equal to the grid-current noise. The higher the grid impedance, the lower the current and voltage at which the valve should be run for optimum performance, but the better the optimum performance will be. The practical limit to grid impedance is set by stray capacity across the transformer secondary, and a suggestion is made in Section 5 for a transformer design having even lower stray capacity than that used in the present equipment.

2. THE LOW-TEMPERATURE TRANSFORMER

2.1 The Behaviour of Mumetal at Low Temperatures

Since no information could be obtained about the behaviour of core materials at temperatures in the region of 20°K, some preliminary

measurements were made on a small 200 turn inductor having a square stack of 0.005 in. mumetal laminations (Inter-Service Lamination Number 439), assembled without a gap, to determine the variation with temperature of core loss, expressed as an equivalent shunt resistance, and inductance. The measurements were made at about 1000 c/s, at which frequency the copper loss of the inductor (even at room temperature) was quite negligible in relation to the core loss; hence the measured dynamic resistance of a tuned circuit, formed by shunting the inductor with a suitable low-loss condenser external to the cryostat, could be taken as a direct measure of the core loss. The measuring level was made low enough (B_{max} about 0.1 gauss) for hysteresis loss to be negligible in relation to eddy current loss. That the hysteresis loss was in fact negligible, was verified at each temperature by increasing the test voltage by a factor of 10, which in all cases produced only a negligible effect on the result.

The inductance at 20°K was found to be approximately 0.30 of its room temperature value, and it varied by less than 1% over the temperature range from 14°K to 20°K. At 77°K (the only intermediate spot reading taken), the inductance was approximately 0.36 of its room-temperature value. Since the test inductor used a core made up from ordinary E and I laminations, the variation in inductance obtained must not be taken as a measure of the variation in the true permeability of mumetal, since such a core inevitably has numerous slight air gaps; these gaps result in the effective measured permeability at room temperature being about 7000, instead of a value of the order of 15,000 such as may be obtained with a strip-wound toroidal core.

The shunt core-loss resistance varied very little with temperature, the change being well under 10% between room temperature and 14°K.

The conclusion is therefore that a mumetal core is perfectly satisfactory at these low temperatures, provided allowance is made in the transformer design for the reduced value of effective permeability obtained.

2.2 The Design of the Low-Temperature Transformer

The low-temperature transformer is very much simpler to design than the room-temperature transformer, for the following reasons:-

(a) Series and shunt loss resistances produce only relatively small Johnson noise voltages because of the low temperature.

(b) Series resistance is, in any case, very small, even in a transformer of the small size shown in Figure 2(a), because of the low specific resistance of copper at such low temperatures.

(c) Stray capacities have negligible effect because of the low values of impedance involved.

The main requirements in the design of the low-temperature transformer are thus:-

(a) The primary inductance must be high enough, in relation to the source impedance, to give an adequate frequency response down to 200 c/s.

(b) The shunt eddy-current loss resistance must be high enough to give only a small loss in output and only a small Johnson noise contribution

(c) The leakage inductance value should be such as to allow the required high-frequency response to be obtained. The value required is closely bound up with the design of the room-temperature transformer, and is discussed in detail in Section 3. It may be mentioned at this stage, however, that an improved high-frequency response may be obtained by making the leakage inductance adequately high, for which reason no sectionalising of the windings is required.

It is found that the required number of turns is determined by condition (c) above, conditions (a) and (b) then being satisfied with large margins to spare. The details of the first transformer constructed, shown in Figure 2(a), are given below. The transformer was designed to suit a source of internal resistance approximately 0.45 ohm, and a nichrome test resistor of this value may be seen in the photograph.

Transformer Details (Low-Temperature Transformer)

CORE — $\frac{1}{4}$ in. stack of 0.005 in. mumetal laminations (Inter-Service Lamination Number 450), assembled without a gap - i.e. fully interleaved.

BOBBIN — Standard bakelite bobbin with moulded-in soldering tags.

SECONDARY — 930 turns of 40 s.w.g. enam. copper wire, layer wound, on inside of bobbin.

PRIMARY — 37 turns of 24 s.w.g. enam. and single rayon covered copper wire, wound on outside of primary, with two thicknesses of 0.005 in. Empire cloth between windings.

The calculated and measured values of various parameters for this transformer are given in Table 1.

TABLE 1

Property	Calculated Value	Measured Value
Ratio	1 : 25.2	-
Primary D.C. resistance at room temperature	0.14 ohm	0.138 ohm
Secondary D.C. resistance at room temperature	55 ohms	53.1 ohms
Shunt eddy-current loss resistance referred to secondary at 800 c/s	184 kilohms	191 kilohms
Main secondary inductance at 1mV, 800 c/s	6.2H	4.5H
Leakage inductance referred to secondary	8.1mH	7.9mH

The formulae used in calculating the values given in the above table were:- (4), (5)

$$R_e = 1.85 \times \frac{\rho_{fe} A n^2}{d^2 l_m} \qquad \ldots (2)$$

$$L = \frac{4\pi n^2}{10^9 (l_m/\mu_o A)} \qquad \ldots (3)$$

$$l = \frac{4\pi l_t n^2}{h} \times \left\{ s + \frac{\Delta_1 + \Delta_2}{3} \right\} \times 10^{-9} \qquad \ldots (4)$$

where:- R_e = Eddy-current shunt resistance in ohms.

ρ_{fe} = Specific resistance of the core material in micro-ohms - cm.*

A = Cross sectional area of magnetic circuit, sq.cms.

l_m = Length of magnetic circuit in cms.

n = Number of turns on winding considered.

d = Lamination thickness in thousandths of an inch.

L = Main inductance of winding having n turns, in Henries.

μ_o = Effective initial permeability of mumetal, taken as 7000 (4).

---

* A value of 42 micro-ohms - cm. is used for mumetal in this formula, though the D.C. value for mumetal is given by Telcon's as 60 micro-ohms - cm. The author has found, as also have the Post Office Research Dept. (4), that a value of 42 gives calculated results which consistently agree well with measured results, whereas 60 gives results which are higher than the measured ones. The adoption of the "A.C. specific resistance" value of 42 micro-ohms - cm. is really a means of allowing for the so-called "residual loss" in mumetal, which is still not properly understood.

l = Total leakage inductance referred to winding having n turns, in Henries.

l_t = Length in cms of insulation between windings, measured round closed (approximately circular) path in direction of wire.

h, s, Δ_1 and Δ_2 - see Figure 5, all dimensions being in cms.

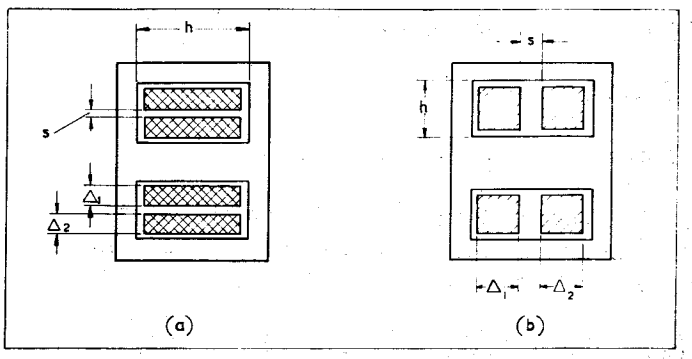

Figure 5

Symbols Used in Formu for Leakage Inductanc

In actual use, the transformer is mounted in a small mumetal screening box to reduce hum pick-up. A mumetal box appears to provide a satisfactory degree of screening at low temperatures, but it would seem that a copper box might also be highly effective, since a large amount of eddy-current shielding should result from the high conductivity of copper at such low temperatures; no experiments have been carried out with copper boxes at low temperatures, however.

3. THE ROOM-TEMPERATURE TRANSFORMER

The factors requiring special attention in the design of the room-temperature transformer have been discussed in general terms in Section 1, where it was shown that the transformer should possess the following attributes:-

(a) A very high ratio of shunt loss resistance to series copper resistance.

(b) A very low value of secondary winding capacity, so that the secondary impedance may be made very high whilst still securing the required high-frequency response.

The copper resistance of a winding may conveniently be expressed in the following form:-

$$r_{cu} = \rho_{cu} \times \frac{n^2 l_t}{A_w k} \qquad \ldots (5)$$

where r_{cu} = Resistance of winding in ohms.

ρ_{cu} = Specific resistance of copper = 1.7 micro-ohms-cm at room temperature.

l_t = Mean length of turn in cms.

n = Number of turns.

A_w = Area of lamination window in sq. cms.

k = Fraction of window area actually occupied by the total cross section of the copper in the winding.

Using also equation (2), the following result is easily derived:-

$$\frac{R_e}{r_{cu}} = \frac{1.85\ \rho_{fe}\ A\ A_w\ k}{d^2\ l_m\ \rho_{cu}\ l_t} \qquad \ldots (6)$$

Since the aim is to obtain as high a value of R_e/r_{cu} as practicable, it is obvious that the laminations should have a high value of ρ_{fe} and that the lamination thickness d should be as small as possible. Rhometal (ρ_{fe} = 90 micro-ohms-cm.) was considered, but was not chosen because it was found that the inductance value obtained with this alloy would have been inadequate for the low-frequency response required. For operating at 800 c/s only, it would, however, have been a more suitable choice, though it is not always easy to obtain rhometal. Having fixed ρ_{fe} and d, and since ρ_{cu} is a constant at room temperature, equation (6) may then be written as the following proportional relationship:-

$$\frac{R_e}{r_{cu}} \propto \frac{A\ A_w\ k}{l_m\ l_t}$$

On multiplying top and bottom by l_m, and remembering that $A.l_m$ is the total volume of the core, this becomes:-

$$\frac{R_e}{r_{cu}} \propto \frac{\text{Core volume} \times A_w\ k}{l_m^2\ l_t}$$

But, for laminations of a particular shape, A_w is proportional to l_m^2, so that the relationship becomes:-

$$\frac{R_e}{r_{cu}} \propto \frac{\text{Core volume} \times k}{l_t} \qquad \ldots (7)$$

In normal transformer practice, where stray capacity is not of overriding importance, as much of the available winding space as possible is filled with copper, with the result that k tends to increase slowly with increasing transformer size, due to the smaller percentage of the space which is occupied by insulation in larger transformers. In the present problem, however, stray capacity is extremely significant, and it is consequently necessary to use smaller values of k than would otherwise be employed; it will be noticed in Figure 2(b) that a considerable amount of air space is left round the windings for this reason.

It is evident from equation (7) that the larger the transformer is made, the higher will be the value of R_e/r_{cu}, assuming a fixed value of k. It may be shown that, for a given core volume, the mean turn-length l_t will be a minimum when a size of lamination is chosen such that the given volume is obtained with a stack thickness about 1.5 times the width of the middle limb. In the present design, however, a square stack was used, but only because the use of a thicker stack would have prevented the transformer from fitting comfortably inside an available mumetal screening box!

The above conclusions may be summarised by saying that, to obtain a high value of R_e/r_{cu}, one should use a large core made of very thin laminations of high resistivity material, with a value of k low enough to keep the stray capacity down to the required figure, but no lower. With constant structural proportions, stray capacity is proportional to the linear dimension of the transformer, but independent of the number of turns; thus, with increasing transformer size, k may have to be reduced to keep the stray capacity low enough, which partly off-sets the advantage otherwise gained by making the transformer larger. By making the lamination thickness d very small, a high value of R_e/r_{cu} can theoretically be obtained without introducing difficulties in keeping down the stray capacities; if an attempt were made to improve markedly on the performance of the transformer design given in this paper, the main line of attack would certainly be to reduce the thickness of the magnetic material, going over to tape-wound toroidal cores if necessary. Some further comments on this aspect are given in Section 6.

So far the problem of deciding the actual number of turns has not been discussed. From equation (6) it is seen that R_e/r_{cu} is independent of the number of turns used; however, it is necessary to have suitable values for R_e and r_{cu} as well as a suitable ratio, and both these

quantities are proportional to n^2. The manner in which the numbers of turns may be chosen so as to make the total Johnson noise introduced by R_e and r_{cu} a minimum will now be considered.

Figure 6 shows the relevant equivalent circuit in its simplest form. Assume that R is much greater than R_o' and that r_{cu} is much less than R_o', which will be true for any transformer satisfactory for the present application. This means that the noise output due to r_{cu} is hardly affected by the presence of R_e and the noise output from R_e is hardly affected by the presence of r_{cu}. Under these conditions, Appendix 1(c) shows that:-

$$\frac{\text{Total mean square noise from } R_e \text{ and } r_{cu}}{\text{Mean square noise from source } (R_o')} = \frac{T}{T_o} \cdot \frac{R_o'}{R_e} + \frac{r_{cu}}{R_o'} \qquad \ldots (8)$$

where T = Room temperature (absolute)
T_o = Source temperature (absolute).

For a given size and shape of transformer, with constant winding volumes, equations (2) and (5) show that $R_e \propto n^2$ and $r_{cu} \propto n^2$.

$$\frac{\text{Total mean square noise from } R_e \text{ and } r_{cu}}{\text{Mean square noise from source}} = \frac{A}{n^2} + Bn^2 \qquad \ldots (9)$$

where A and B are constants.

The first term in equation (9) represents the mean square noise from R_e and the second term represents the noise from r_{cu}; these two terms appear as the two dotted lines in Figure 7. Since the mean square noise in this graph is in arbitrary units, and since the numbers on the abscissa are merely proportional to the number of turns on the windings, the position of the lines conveys no information, only their slopes being significant. The full-line curve is the sum of the two dotted lines and shows the manner in which the total noise contributed by the transformer varies with the number of turns n. It is clear that the minimum total noise occurs when the noise contributions from R_e and r_{cu} are equal; thus, from equation (8), n should ideally be chosen to make $R_e/R_o' = R_o'/r_{cu}$. (Since the curve has quite a flat minimum, the increase in noise is negligible if the number of turns is made up to 20% less than the optimum and, because a reduction in the number of turns makes the transformer easier to wind, the transformer constructed has slightly less than the optimum number of turns.)

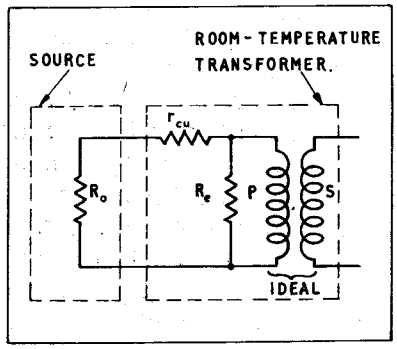

Figure 6

Simple Equivalent Circuit showing Transformer Losses

R_o' = Source resistance
r_{cu} = Total winding resistance
R_e = Eddy current resistance
(All referred to primary of room-temperature transformer)

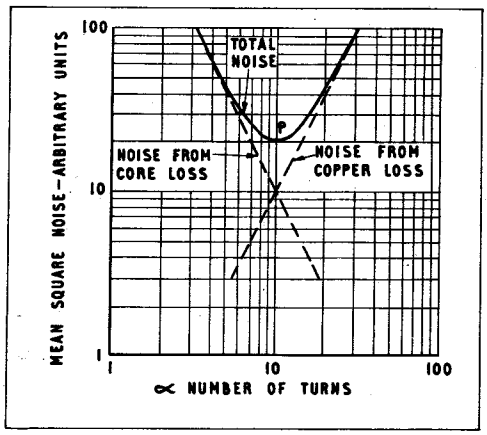

Figure 7

Variation of Noise from Transformer Losses with Number of Turns

The first room-temperature transformer constructed, which is the one illustrated in Figure 2(b), gave measured values of its various parameters which agreed well with previous calculations, with the exception of the shunt loss resistance which was only about half the calculated value. This result was at first very puzzling, since numerous previous transformers wound by the author had given measured shunt resistance values much closer to the calculated values, using formula (2). A shorted turn was at first suspected, but was thought to be very unlikely in view of the care taken in winding the transformer and the good condition of the wire used. However, even though the shunt resistance was only half the calculated value, it was still sufficiently high to enable a noise factor of just under 3 dB to be obtained with the source at 20°K, which was the figure initially aimed at, and for this reason the transformer was put into service as it stood. Insulation losses in the paxolin (phenol formaldehyde) bobbin were later investigated, and measurements of the impedance between the two windings, made with the help of an E.M.I. (Blumlein) in situ Bridge at about 1.59 kc/s, showed that the power factor of the insulation was about 13%; a value found, on referring to the literature[6], to be typical of paxolin. Since this power factor was of the right order to explain the discrepancy in the measured and calculated shunt resistance, another transformer was made, identical with the first except for the use of a polystyrene bobbin and terminal board. The new transformer, called No. 2, gave a measured shunt resistance very close to the calculated value, proving that the paxolin used in No. 1 was an insufficiently good insulator for the purpose.

Transformer Details (Room-Temperature Transformer)

CORE — 3/4 in. stack of 0.005 in. mumetal laminations (Inter-Service Lamination Number 401A), assembled without gap - i.e., fully interleaved.

PRIMARY — Two sections, wound in reverse directions, each having 84 turns of 24 s.w.g. enam. and single rayon covered wire. Centre tap brought out.

SECONDARY — 10,000 turns of 44 s.w.g. enam. in $\frac{3}{8}$ in. wide slot between the primary sections. One layer of 0.005 in. Empire cloth every 1000 turns. Turns wound neatly but not in true layers.

The calculated and measured values of various parameters for the two transformers are given in Table 2.

TABLE 2

Property	Calculated Value	Measured Value	
		Transformer No. 1	Transformer No. 2
Ratio	1 : 59.6	-	-
Primary D.C. resistance at room temp., total	1.3 ohms	1.34 ohms	1.32 ohms
Secondary D.C. resistance at room temp.	4.0 kilohms	3.92 kilohms	4.32 kilohms
Shunt eddy-current loss resistance referred to primary, at 800 c/s	20.2 "	10 "	20.5 "
Shunt eddy-current loss resistance referred to secondary, at 800 c/s	72 megohms	36 megohms	73 megohms
Main primary inductance at low level	0.57H	0.56H	0.60H
Leakage inductance referred to primary	0.74mH	0.76mH	0.77mH
Leakage inductance referred to secondary	2.64 H	2.71 H	2.75 H
Secondary stray capacity	< 50 pF	37 pF	27 pF

With a source impedance of 300 ohms referred to the primary (= 1.06 megohms referred to the secondary), the measured results given in Table 2 for the better of the two transformers yield figures for R_o'/R_e and r_{cu}/R_o' of 0.0147 and 0.0085 respectively. Thus, from equation (8), the mean square eddy-current noise is greater than the mean square copper resistance noise by a factor of 0.0147/0.0085 - i.e., by 1.73 times. This condition corresponds with the point "P" in Figure 7, and is thus highly satisfactory.

The primary inductance value (0.56H), measured at low level on transformer No. 1, corresponds to a low-frequency response, when fed from a 300 ohm resistive source, which is 3 dB down at 85 c/s, and transformer No. 2 is slightly better. When the 300 ohm resistive source is replaced by the low-temperature transformer and fractional-ohm source, allowance must be made, in estimating the frequency response, for the shunting effect of the

secondary inductance of the low-temperature transformer; taking this as 1.35H when at low temperature, the total parallel inductance is 0.40H, giving a response 3 dB down at about 120 c/s. The requirement, mentioned in Section 2.2, that the response should not be more than 3 dB down at 200 c/s, is thus satisfied with a good margin to spare.

The method used for measuring the effective stray winding capacity across the secondary was as follows. The transformer was mounted in its mumetal screening box, with the core, the inside of the secondary and one end of the primary all earthed to the box; initially no connection was made to the outside secondary lead. The primary was fed from an oscillator with a resistance of about 1 kilohm in series, and a valve voltmeter arranged to indicate the A.C. voltage across the primary. On tuning the oscillator, a frequency was found at which the primary voltage fell to a fairly sharp minimum, this being the frequency of series resonance between the leakage inductance, referred to the secondary, and the stray capacity of the secondary winding. By plotting the reciprocal of the square of the resonant frequency against the value of known capacities added across the secondary, a straight line graph was obtained, the intercept of which on the capacity axis gave the required stray capacity of the secondary winding. It may be noticed that the stray-capacity value obtained with transformer No. 2 is considerably less than that for No. 1, and it is believed that this is the result of the fact that polystyrene has a dielectric constant of about 2.6 as against a value of about 5 for paxolin; this is another good reason why polystyrene is preferable.

The relevant equivalent circuit from the point of view of the high-frequency response is shown in Figure 8(a). C_{sec}, the

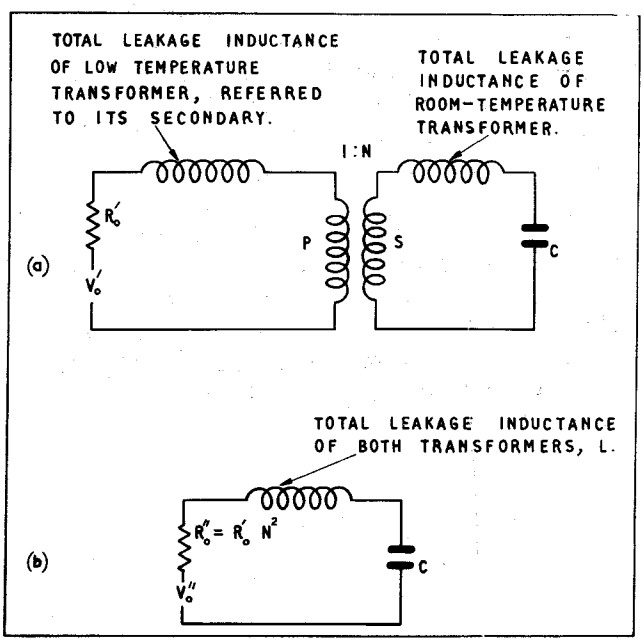

Figure 8

Simple Equivalent Circuits for Determining H.F. Response

total secondary stray capacity, consists partly of that inherent in the transformer itself, as given in Table 2, and partly the additional capacity inevitably resulting from connecting the transformer to the input valve. Some information given to the author by C. G. Mayo, relating to B.B.C. microphone transformers, made it reasonable to assume, with the construction shown in Figure 2(b), that C_{sec} would be about 50 pF provided only a short lead were used from the outside of the secondary winding to the top-cap grid of the pentode input valve. By referring all values to the secondary side of the transformer shown in Figure 8 (a), the simpler equivalent circuit of Figure 8(b) is obtained. The object is to choose the turns ratio N and the total leakage inductance L so as to ensure that, as stipulated in Section 2.2, the response at 3200 c/s shall not have fallen off relative to that at lower frequencies by more than 3 dB. It is a good practical rule to make the leakage inductance L such as to resonate with the stray capacity C at the upper working frequency, which may be taken as 4 kc/s in the present case to allow a reasonable margin. Taking C as 50pF, this gives L = 31.6 H. The turns ratio N must then be chosen to make the Q of the Figure 8(b) circuit suitable; too high a Q will give a peak in the frequency response just below 4 kc/s, while too low a Q will cause the response to start falling off slowly at frequencies much below 4 kc/s. A suitable value of Q to adopt is Q = 0.8, which corresponds to:-

$$R_o' N^2 = 1.25 \times \frac{1}{2\pi f_o C}$$

where f_o is the "cut-off frequency" (= 4 kc/s). Putting C = 50 pF gives $R_o' N^2$ = 1.0 megohm, so that, with R_o' = 300 ohms, N is 1 : 57.6. Since this aspect of the design is not highly critical, N was made as near as possible to the round figure of 1 : 60, with 10,000 turns on the secondary and 168 on the primary. The actual ratio being 1 : 59.6, the required leakage inductance of 31.6 H referred to the secondary becomes 8.9 mH referred to the primary. It was found to be inconvenient to obtain a leakage inductance value as high as this in the room-temperature transformer, the value actually obtained being 0.76 mH, but it was a simple matter to obtain the difference in the low-temperature transformer - this is the reason for the requirement, stated in Section 2.2, that the leakage inductance of the low-temperature transformer, referred to its secondary, should be 8.1 mH.

The design criterion given by equation (10) results in a theoretical response which is up by 0.2 dB at 0.5 f_o, returns to 0 dB at 0.65 f_o and is 2 dB down at f_o. The frequency response actually obtained in practice, with a 0.45 ohm source at 20°K, is shown in Figure 9, curve (a), and will be seen to be in good agreement with theory. Curve (b) shows the response obtained with a 300 ohm resistive source feeding the room-temperature transformer directly, the poorer high-frequency response being due to the absence of the low-temperature transformer leakage inductance.

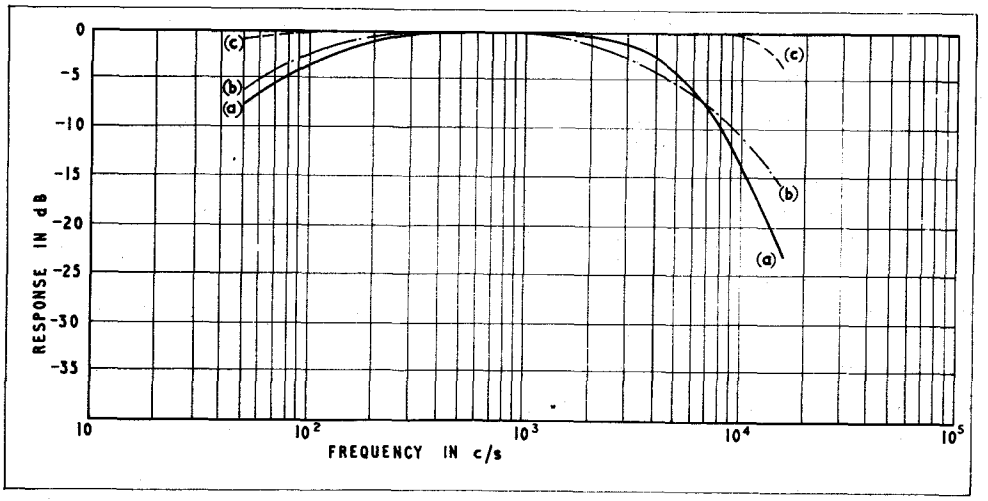

Figure 9

Measured Frequency Response
Curves for Transformers and Amplifier

(a) 0.45 ohm source and low temperature transformer at 20°K
(b) 300 ohm source) Direct to room-temperature
(c) 82 ohm source) transformer

(Room-temperature transformer No. 1 used)

Curve (c) is for an 82 ohm source feeding the room-temperature transformer directly; the resonant frequency of the secondary stray capacity, taken as 50 pF, and the leakage inductance of the room-temperature transformer by itself, is 13.7 kc/s, and 82 ohms is the value of R_o' which then satisfies equation (10). The corresponding value referred to the secondary is 290 kilohms.

It is the normal practice in good-class input transformers, employing balanced two-wire input feed, to insert an electrostatic screen between the primary and secondary windings, to prevent the transfer, via the inter-winding capacity, of push-push or "longitudinal" interference picked up by the input cable. For the present application, however, it was felt that the insertion of copper-foil screens would be likely to cause a significant reduction in the shunt loss resistance of the transformer, due to the flow of eddy currents, induced by the leakage flux, in the screens. For this reason, and in view of the fairly short screened input cables used, no screens were fitted, but no

serious trouble from interference pick-up on the input cable has been experienced under normal working conditions.

4. THE AMPLIFIER CIRCUIT

The amplifier circuit has already been outlined in Section 1. Some of the details, which may be of interest, will now be described briefly.

As mentioned in Section 1, it was decided , in order to be sure of getting adequately low grid current, to use an ME1400 input valve, with $V_a = V_{g2} = 45$ V and an anode current in the region of 100 μA. Under these conditions, the slope is about 0.3 mA/V, and a high value of anode load must be used to obtain a good stage gain. With a supply voltage of 170V at the top end of the anode load, the anode current must remain stable within quite close limits if the anode voltage is to remain reliably clear of the bottoming region and yet not much greater than 45V. This requirement is met by means of a D.C. negative feedback circuit between anode and grid, which, in conjunction with a reference voltage supplied by a 9V. grid-bias battery, automatically maintains the anode voltage within a few volts of 45 V despite changes in valve characteristics and supply voltages. This negative feedback is rendered inoperative at signal frequencies by suitable decoupling arrangements.

The switching circuit employed for the overall feedback network has been arranged so as to avoid the use of resistor values of a fraction of an ohm and to ensure that small amounts of switch contact resistance cannot appreciably affect the feed-back factor.

On the $\times 10^5$ gain setting, the available valve gain limits the amount of overall feedback to about 20 dB, but at lower gain settings the amount of overall feedback is intentionally reduced, in the interests of obtaining adequate stability margins, by the application of local feedback round V_2. By controlling the forward gain in this manner, rather than by inserting passive attenuation, the noise factor of the amplifier is not appreciably increased at low gain settings. It will be seen that a capacitor is shunted across the local feedback network of V_2 on each range; the object of this is to ensure that the overall loop gain shall be attenuated sufficiently gradually to give an adequate phase margin. Because of the small capacity values involved at the higher gain settings, it is essential to adopt precautions to prevent stray capacities upsetting the intended results; these precautions involve mounting the feedback components through holes in a screen between the grid and anode circuits of V_2, and using a shorting section on the switch to earth the networks intended for lower gain settings when higher gain settings are in use. It is on the $\times 10^5$ range that it is most important to keep anode-to-grid capacity to a minimum - even 1 pF would have a large effect on this range - so that, on this range only, a purely passive network, consisting of 100 pF and

150 kilohms across V_1 anode load, is used to control the loop gain attenuation. Figure 10 illustrates the principles involved; curve (a) shows how the loop gain of the amplifier is attenuated without the addition of any special controlling elements, curve (b) shows the attenuation of loop gain as modified by local feedback round V_2 on the x 10^2 gain setting, and curve (c) shows the gain with overall feedback in operation on this range.*

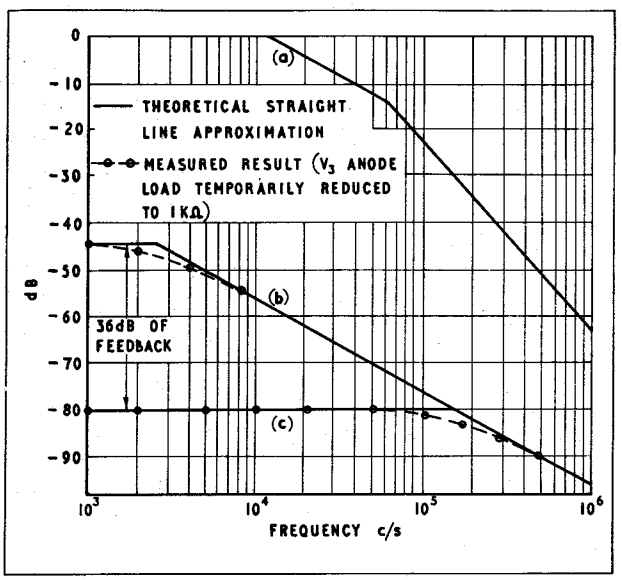

Figure 10

Response Curves for x10^2 Range

Curve (a) Overall loop gain without addition of special controlling elements
Curve (b) Overall loop gain with local feedback on V_2
Curve (c) Response with overall feedback

A problem of very similar nature to the above is also involved at low frequencies; the loop gain at medium frequencies must be attenuated, with falling frequency, in a

---

* The test waveform was applied direct to the grid of V_1, and the anode load of V_3 was temporarily made 1 kilohm.

sufficiently gradual manner to avoid too much phase shift and thus to secure an adequate phase margin. This is achieved by suitable proportioning of the interstage time constants and the screen and cathode time constants.

To illustrate the adequate stability achieved, the step function response* on the x 10^2 range is shown in Figure 11. The amount of overall feedback on this range is 36 dB. The step function responses on the other ranges show a comparable degree of stability.

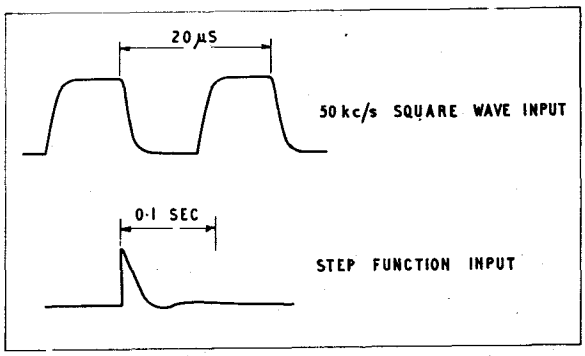

Figure 11

Amplifier Transient Response Waveforms (Excluding transformers)

By means of switch S_2, the anode of V_3 may be connected either to an 800 c/s tuned circuit, having a Q of approximately 40, or to a simple resistance load. The effective A.C. value of the latter is 40 kilohms, and the dynamic resistance of the tuned circuit at resonance is made of the same value. All contacts on switch S_2 are of the make-before-break variety, and the arrangement used ensures that no D.C. switching transient reaches the output terminal when changing over from the "Tuned" to the "Wideband" setting and vice-versa. The "off" positions of S_2 are also useful for shorting the amplifier output so as to avoid switching transients when operating the gain switch S_1, such transients being very undesirable if delicate recorders or thermocouple instruments are used at a later stage in the system.

The inductor used for the output tuned circuit has a toroidal dust core with an effective permeability of about 120, which gives good stability and absence of sensitivity to stray magnetic fields. A separate winding is provided for the output, instead of employing a coupling condenser direct from the valve anode, since this gives the advantage that ripple and other fluctuations in the H.T. supply to the anode of V_3 do not appear at the amplifier output terminal.

---

* See footnote page 24.

The method used for obtaining a small range ($\pm$ 20 c/s) of variable tuning is to change the tuning capacity in steps by means of the 12 - position switch S_3. Though this arrangement is reasonably satisfactory for the present purpose, it is felt that a truly continuous tuning adjustment would really be preferable. A satisfactory solution could probably be obtained by using the variometer principle, in the form of a laminated stator carrying most of the turns in series with a laminated rotor carrying a small percentage of the turns. This idea has not been pursued, however, and the author would be very interested to hear from any reader who has produced a practical variable-frequency tuned circuit suitable for applications of the sort here described and of a purely passive nature.

Though D.C. heater supply is normally used with this amplifier, provision is made for the alternative use of A.C. It is interesting to note, that although 800 c/s is the 16th harmonic of 50 c/s, no evidence of an output component at this frequency can be detected, with A.C. heater supply, on tuning the output circuit through the exact mains-harmonic frequency; it would therefore seem that 50 c/s heater supply is really quite satisfactory in a selective amplifier of the type described, even when used for noise measurements of the most exacting nature. It will be seen that special arrangements are used in the heater circuit under A.C. conditions, involving a double-screened heater transformer and a double-screened lead. This system renders the hum level almost independent of reasonable amounts of heater-cathode leakage in the input valve, despite the use of cathode-injected feed-back. On the "wideband" setting of S_2, the hum-level with A.C. heater supply, though satisfactorily low by normal standards, is too great to enable satisfactory noise measurements to be made, and D.C. supply must then be used.

The room-temperature transformer is mounted inside two mumetal screening boxes, though experience in use has shown that it would really have been preferable to have had three boxes; with two boxes only, on the "wideband" setting, a noticeable hum output appears, due to transformer pick-up, unless all mains transformers, etc, are kept a yard or two away from the input transformer. To reduce the sensitivity of the apparatus to vibration and acoustic waves, to which the input transformer was found to respond, the space between the two mumetal boxes is filled with Wood's metal, making a massive and rigid structure which is then suspended in sorbo rubber. The input valve is mounted inside a substantial brass can with a screw lid, the can being fixed rigidly to the side of the outer mumetal box and being thus suspended in sorbo rubber with the box. These measures have provided an excellent degree of freedom from microphony.

The whole amplifier circuit is completely enclosed inside the

aluminium structure of the unit, the H.T. and L.T. supply leads enterin via a screened R.F. interference suppressor unit. The latter was adde after it was found that spurious outputs were obtained when a sparking-coil vacuum-leak detector was operated in an adjacent laboratory, and effected a large improvement. On working the spark device within a yard of the amplifier, however, some spurious output still resulted; since the fitting of a 3.9 kilohm grid stopper produced a further large improvement, it would seem that quite high radio frequencies were involved. For all practical purposes the amplifier is now quite satisfactorily immune from response to such spurious interference, but to get rid of all trace of response under conditions of very intense R.F. interference appears to be quite a difficult problem.

With the source at 20°K, the r.m.s. source noise appearing at the output terminals, with the tuned circuit switched in and a gain of $x10^5$, is about 15 mV; this is sufficiently high to allow the use of an ordinary broadband audio-frequency amplifier in the following part of the system, without obtaining a significant noise contribution from this latter amplifier. Though the ideal arrangement, for feeding from the unit here described to the following amplifier, would be to use a twisted and screened balanced line, it has been found in practice that no trouble, in the form of interference pick-up by the inter-unit wiring, is experienced with the unbalanced output circuit employed, provided one takes care that the only significant connection between the earth lines of the two units is via the braiding of the coaxial signal lead. If the two amplifiers are operated from a common power pack, a resistor of about 100 ohms should be included in series with the H.T. - terminal of the broadband amplifier, so as to ensure that, on plugging in the signal cable between the units, it makes a much lower resistance earth connection between them than that occurring via the H.T. - wiring. In this way the formation of an effective wiring loop for picking up magnetically-induced interference is avoided.

The under-chassis layout of the amplifier is shown in Figure 12. Each valve is mounted in its own screened compartment on the top of the chassis, the screening partitions under the chassis being staggered with respect to those on top, so as to allow an open lead to be taken from the anode circuit of one valve to the grid circuit of the next without introducing anode-to-grid capacity across the first valve considered. With this arrangement, no screened leads are necessary in the interstage wiring and stray capacities are kept to the minimum. The remaining precautions taken are the avoidance, as far as practicable, of wiring loops in the input circuit (especially on the primary side of the input transformer) [3], the use of only the best quality components in good condition throughout, and the avoidance of any conditions likely to lead to erratic contacts anywhere in the circuit. The result has been that during many months of use there has never been any evidence of spurious noise, crackling, etc. due to causes lying within the amplifier.

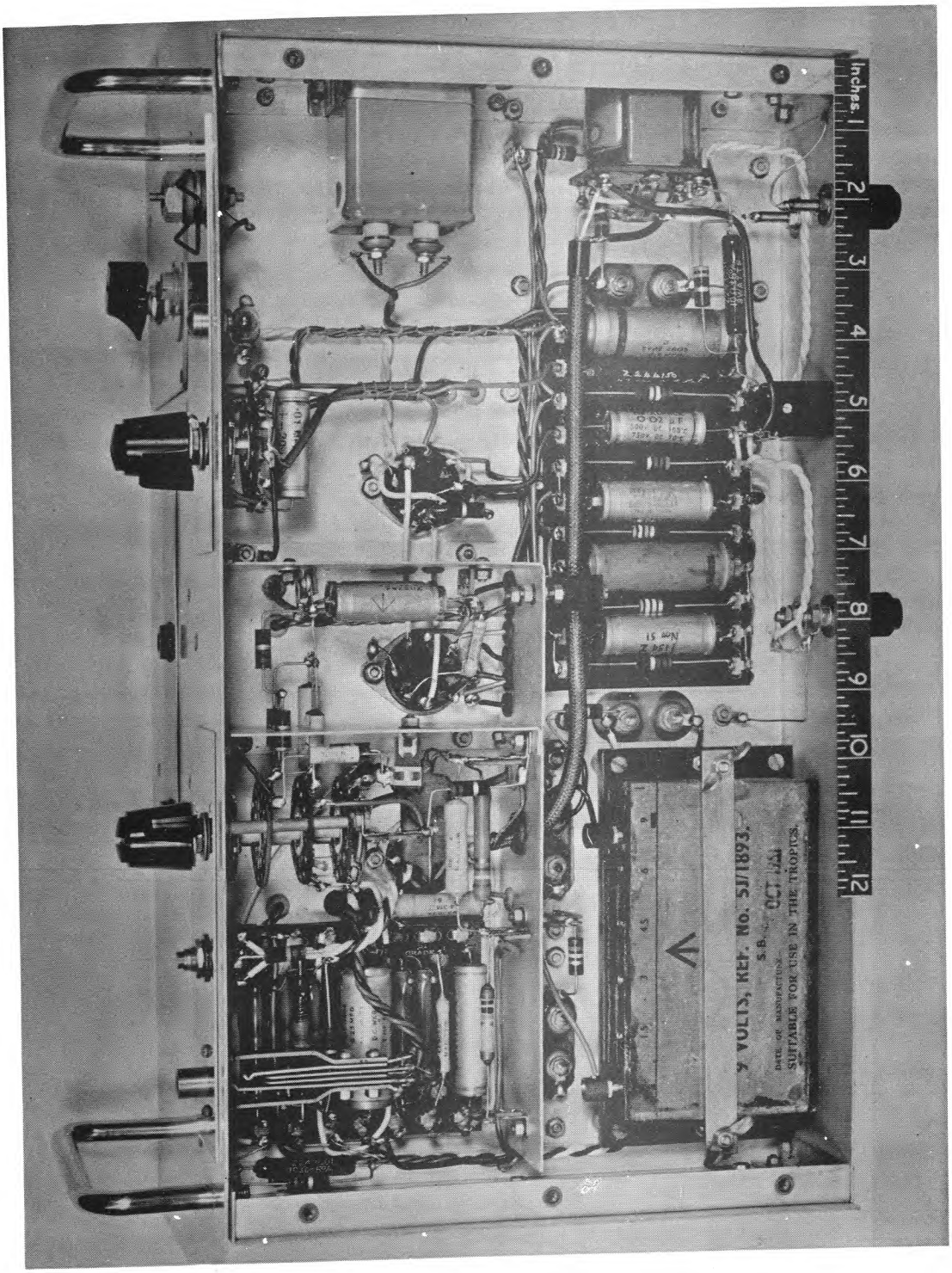

Figure 12

Under-Chassis Layout of Amplifier

5. CONSIDERATION OF METHODS FOR OBTAINING A STILL LOWER NOISE FACTOR

5.1 General

In Section 1, it was mentioned that, when grid-current noise is a significant contribution, it is by no means obvious that the lowest noise factor is necessarily obtained by stepping up to the highest possible grid impedance and adjusting the valve operating conditions appropriately. In the present section, the variation of grid current and equivalent shot and partition noise resistance with valve operating conditions will each be considered, leading to a method of designing equipment of the present type for minimum noise factor. It will be shown that the total valve noise can be made so small in relation to the noise contributed by the losses in a transformer such as that described in Section 3, that it is only by designing an improved transformer that the full benefit of the reduced valve noise can be obtained. Suggestions for an improved design of room-temperature transformer will be made.

It is believed that a noise factor not greater than 1 dB, with the source at 20°K, should be attainable by the improved methods described.

5.2 Variation of Equivalent Shot and Partition Noise Resistance with Operating Conditions

A theoretical formula, which appears to have very wide acceptance,(2) for shot and partition noise in pentodes with oxide-coated cathodes, is:-

$$R_{eq} = \frac{2.5}{g_m} \times \frac{I_a}{I_a + I_{g2}} \times \left[1 + 8 \frac{I_{g2}}{g_m}\right] \quad \ldots (11)$$

where:- R_{eq} = Equivalent noise resistance in kilohms

g_m = Mutual conductance in mA/V

I_a = Anode current in mA

I_{g2} = Screen current in mA.

The second term inside the brackets in equation (11) represents the extra contribution due to partition noise.

The above formula is properly applied, however, only when the anode current of a valve is limited mainly by the space-charge mechanism and where the velocity of emission of electrons has only a minor effect. Under such space-charge-limited conditions there is a pronounced minimum in the potential distribution between cathode and anode, this minimum lying close to the cathode in the grid-cathode space and being responsible for the peculiar phenomenon of "space-charge smoothing of shot

noise fluctuations". When, on the other hand, a valve is operated at abnormally low anode and screen voltages and currents, there is no such potential minimum within the grid-cathode space and a retarding field* exists throughout the grid-cathode space, rendering the mechanism of space charge smoothing ineffective. Under these conditions, the same basic theory that led to equation (11) now leads to the simpler result:-

$$R_{eq} = \frac{20\ I_a}{g_m^2} \qquad \ldots (12)$$

Some measurements were made on an ME1400 pentode, at a fixed grid bias of - 2.0 V, to determine the variation of g_m with I_a and I_{g2}, V_{g2} being adjusted as required. From these results R_{eq} was determined, using formulae (11) and (12), and the curves shown in Figure 13, curves (a) and (b) respectively, were plotted.

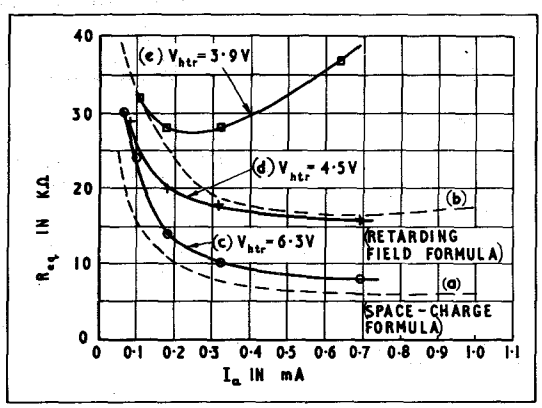

Figure 13

Variation of Equivalent Noise Resistance with Anode Current for Pentode-connected ME 1400

Broken lines show theoretical curves.
Full lines show experimental curves.

---

* i.e., an electrostatic field such that the force exerted on an electron in the field is in the opposite direction to its velocity of emission from the cathode.

The valve was then inserted in the amplifier circuit of Figure 3, the input stage being temporarily modified to enable the operating conditions to be adjusted as required. With the 800 c/s tuned circuit in operation, the output was fed to a linear rectifier and pen recorder. Provision was made for inserting resistances of 0, 30 and 50 kilohms in the grid circuit and, for each set of valve operating conditions, recordings were made for a few minutes with each of the above resistance values in circuit. From these recordings, the mean square noise output, in arbitrary units, was deduced, and it was verified that, in every case, the mean square noise varied linearly with the value of resistance inserted in the grid circuit, i.e., that the three points obtained for the three values of grid resistance lay on a straight line. (The fact that good straight lines were obtained provided a means of checking that genuine noise was being measured, and that there was no significant component due to interference pick-up when the grid circuit impedance was increased). The negative intercepts of these straight line graphs on the resistance axis gave the values of R_{eq} as determined experimentally. The results have been plotted as curves (c), (d) and (e) for three values of heater voltage. It will be seen that curve (c), for $V_{htr} = 6.3$ V, lies between the two theoretical curves, tending towards the "space-charge-limited" curve at higher anode currents and towards the "retarding field" curve at lower anode currents, and it may therefore be said that the measured curve is in reasonable agreement with the theory. The large increase in noise with reduction of heater voltage, at higher anode currents, is rather difficult to explain, however, since even with $V_{htr} = 3.9$V the available cathode emission is much greater than the actual anode current used. A further experimental observation is that the equivalent noise resistance, for an anode current of 170 μA, is approximately twice as great with a negative grid-bias of 4 V. as with the bias of 2 V. used for the rest of the measurements; this can be explained, at least qualitatively, by the reduction of g_m which occurs with large negative bias and high screen voltage.

Inasfar as the theory used has taken no account of flicker noise, the satisfactory experimental agreement obtained would seem to indicate that, at 800 c/s and over the anode-current range investigated, flicker noise does not contribute very significantly to the total valve noise if a good specimen of valve is used. This result is in agreement with the prediction of G. R. Nicoll, to whom the author is much indebted for helpful advice on the valve noise problem. In an unpublished theoretical and experimental investigation by Nicoll and Warner,* carried out in 1951, the following formula was given for the equivalent noise resistance of a pentode, including flicker noise:-

$$R_{eq} = \frac{2.5}{g_m} \times \frac{I_a}{I_a + I_{g2}} \times \left\{1 + \frac{I_a}{I_o}\right\} \times \left\{1 + \frac{8I_{g2}}{g_m}\right\} \quad \ldots (13)$$

where I_o is defined as the value of anode current at which flicker noise contributes half the total mean square valve noise; I_o varies

---

* Of R.R.E.

considerably from one valve sample to another at a given frequency, and is also approximately proportional to frequency.

This formula, though not absolute, in the sense that I_o requires to be determined experimentally for one set of operating conditions, is useful insofar as it enables the variation in flicker noise for any change in the operating conditions to be determined. A satisfactory degree of agreement with experimental results was obtained.

5.3 Variation of Grid Current with Operating Conditions

It will be assumed, in the following treatment, that sufficient negative bias is used to ensure that grid current due to the collection of electrons by the grid, is negligible; a grid bias of - 2.0V is sufficient to fulfil this condition.

Reference (2) states that, in a triode-connected valve which has been aged* for a few days and selected for low grid current, the reverse grid current is found to obey approximately the relationship:-

$$I_{g1} = K I_k V_a^2 \qquad \ldots (14)$$

where K is a constant varying considerably from one valve to another, and the grid current is "reverse" grid current - i.e., in the opposite direction to that caused by the collection of electrons by the grid. No theoretical explanation for this formula is given in the Reference, nor is there any indication how the formula should be modified to suit pentode operation with V_a not equal to V_{g2}.

Several measurements were therefore made on an ME1400 valve operated as a pentode, with a heater voltage of 5.0 V; it was found that all the results obtained agreed with the following empirical formula, within about $\pm$ 20%:-

$$I_{g1} = K I_k V_a V_{g2} \qquad \ldots (15)$$

where $K = 1.0 \times 10^{-11}$

I_{g1} = Grid current in amps.

I_k = Cathode current in amps.

---

* i.e., run continuously under normal working conditions.

V_a = Anode voltage in volts.

V_{g2} = Screen voltage in volts.

Two of the results obtained are shown as graphs in Figure 14.

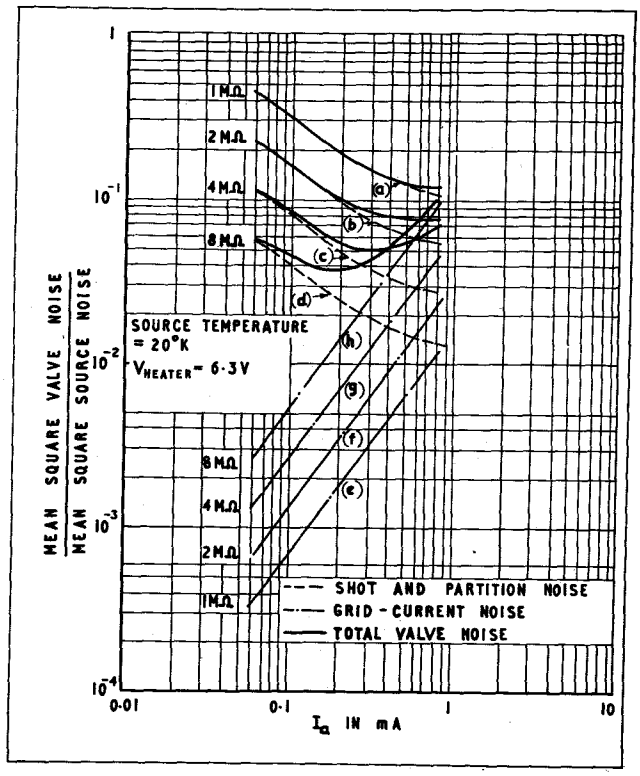

Figure 14

Valve-Noise Characteristics

No satisfactory explanation of equation (15) has been found, but, as a result of a discussion with A.C. Prior of R.R.E., the following facts were brought to the author's attention:-

(a) The vacuum pressure in any good modern receiving valve, after ageing for a few days, should not exceed 10^{-8} mm. of mercury, most of the gas left in the valve after manufacture being absorbed by the cathode during the ageing process.

(b) At such a low gas pressure, ionization of the gas could not account for nearly as much grid current as is found in practice.

(c) Another mechanism for the production of reverse grid current, [7], [8] apparently first suggested by Prof. W. B. Nottingham of M.I.T., is that, when electrons bombard the anode of a valve, soft X-rays are produced which then cause the emission of photo-electrons from the grid. In reference (8), some good evidence is given that this mechanism is in fact mainly responsible for the residual grid current at pressures below 10^{-8} mm of mercury, and the relation between grid current and anode voltage is a simple power law with an index between 1.5 and 2.0.*

After the conclusion of the above grid-current measurements on an ME1400, J. Canning and S.J. Widdows made some grid-current measurements on 12 CV2135's and 12 CV138's, triode connected and with a heater voltage of approximately 6.3 V. A grid bias of - 2.0 V. was used throughout, and appropriate values of anode voltage were applied to give cathode currents of the order of 10, 2.5 and 0.5 mA for each valve. The grid current was measured at each of these cathode currents, both when the valves were new, and after ageing for 100 hours. With most of the valves, the ageing process gave a reduction in grid current of two or three times, and it was then found that the measured grid current values fitted an equation of the same form as (14) sufficiently closely for the equation to be of practical utility. On determining the values of K by substituting the figures for I_k = 2.5 mA in equation (14), for each valve, it was found that, with the exception of two valves out of the 24 tested, K was always within the limits + 100% to - 50% of the value determined by the author for an ME1400.

The above results suggest that formula (14), and probably (15) also, with K = 1.0×10^{-11}, may be used to give the order of magnitude of grid current in any small receiving valve which has been well aged, but tests on much larger numbers of valves would be necessary before any rigid conclusions could be reached.

---

* No theoretical justification for the observed power law is given. Prior has pointed out that the <u>fraction</u> of the energy of an electron converted to X-rays is proportional to the atomic number Z of the target element multiplied by the energy of the electron - i.e., it is proportional to ZV, where V is the target voltage. Hence the total energy converted to X-rays is proportional to ZV^2 x (number of electrons). On the assumption, the justification for which is rather doubtful, that the number of photo-electrons emitted from the grid is proportional to this total X-ray energy, the above relationship leads directly to an equation of the same form as equation (14), i.e.

$$I_{g1} = K I_k V_a^2$$

5.4 Variation of Total Valve Noise with Operating Conditions

In designing equipment of the present type for minimum noise factor, the aim, as far as valve noise is concerned, is to obtain the smallest possible value of

$$\frac{\text{Mean square shot-and-partition noise} + \text{Mean square grid-current noise}}{\text{Mean square source noise}}$$

The initial calculation will be based on a source temperature of 20°K and a room temperature of 290°K, with an ideal transformer system stepping up to 1 megohm. The mean square noise from 1 megohm at 20°K is the same as that from a resistance of 1 megohm x (20/290), i.e. 69 kilohms at room temperature. Hence, under these conditions:-

$$\frac{\text{Mean square shot-and-partition noise}}{\text{Mean square source noise}} = \frac{R_{eq}}{69} \qquad \ldots (16)$$

where R_{eq} = equivalent room-temperature resistance, in kilohms, representing shot and partition noise.

The measured values of R_{eq}, as given in Figure 13, curve (c), may then be used in equation (16) to obtain Figure 14, curve (a). On increasing the transformer secondary impedance to 2 megohms, which requires the turns ratio to be multiplied by $\sqrt{2}$, the r.m.s. source noise at the secondary is multiplied by $\sqrt{2}$ and the mean square noise by 2; since the valve noise (shot and partition only) is unaffected by increasing the transformer ratio, it follows that the curve corresponding to Figure 14, curve (a), for a secondary impedance of 2 megohms, is the same as curve (a), but shifted up by a factor of 2. Curves for 4 megohms, 8 megohms, etc. may thus easily be drawn.

The basic formula relating to grid-current noise is*:-

$$\overline{i_{gn}^2} = 2\,e\,I_g\,\delta f \qquad \ldots (17)$$

where:- $\overline{i_{gn}^2}$ = Mean square value of shot-noise component of grid current.

e = Charge of an electron = 1.60×10^{-19} Coulomb.

* This formula can be applied correctly to determining the total grid current noise only if I_g is caused by a single significant effect; e.g., if $I_g = 0$ due to balancing of forward and reverse components, each component will produce shot noise and the total grid current shot noise (mean square) will be the sum of the mean square values due to each component.

I_g = Mean grid current in amps.*

δf = Noise bandwidth in c/s.

The mean square grid current noise voltage at the grid is:-

$$2 e I_g \delta f (R_o")^2$$

where $R_o"$ is the source resistance referred to the grid.

Hence

$$\frac{\text{Mean square } I_g \text{ noise}}{\text{Mean square source noise}} = \frac{2 e I_g \delta f (R_o")^2}{4 k T_o R_o" \delta f}$$

$$= \frac{e I_g R_o"}{2 k T_o} \quad \ldots (18)$$

where k is Boltzmann's constant and T_o is source temperature. With $R_o"$ = 1 megohm and T = 20 K, formula (18) becomes:-

$$\frac{\text{Mean square } I_g \text{ noise}}{\text{Mean square source noise}} = 2.9 \times 10^8 I_g \quad \ldots (19)$$

Using formula (15) for I_g, (19) may be evaluated for various values of I_k, taking V_{g1} = -2.0 V and using the minimum value of V_a consistent with keeping comfortably clear of bottoming, V_a was taken as 40 V at I_k = 50 μA, and increased gradually to 60 V at 1.5 mA. In this manner, Figure 14, curve (e) was derived; other curves, for $R_o"$ = 2, 4, 8 megohms may then be drawn as shown. The variation of (total mean square valve noise/mean square source noise) with anode current, for various grid circuit impedances, may then be obtained by adding the ordinates of the appropriate pairs of curves; these total noise curves are shown full-line in Figure 14. It will be seen that, provided the valve is operated at the most suitable value of anode current, the total valve noise becomes smaller and smaller in relation to the source noise as the secondary impedance of the input transformer is made higher and higher. It should be noted that this is so only because the two sets of curves are of unequal steepness.

It will be seen that by stepping up to 4 megohms, and running at an anode current of about 0.35 mA, the total mean square valve

---

* See footnote on page 35.

noise is about 0.05 of the mean square source noise with the source at 20°K. Assuming a noiseless transformer, the equipment would then give a noise factor of 3 dB with the source at 20°K x 0.05, i.e., 1°K, and the noise factor with the source at 20°K would be $10 \log_{10} 1.05$, i.e., about 0.22 dB. It is almost certain that, in practice, the limiting factor would turn out to be the transformer design, and calculations based on the analysis in Appendix 1 show that a ratio of shunt to series loss resistance of about 1.75×10^6 would be required to make the transformer noise about equal to the amplifier noise, and thereby to achieve a total noise factor in the region of 0.4 dB.

With a transformer of the same size as that used in the equipment described in this paper, the required improvement in shunt-to-series-loss resistance ratio could in theory be obtained by reducing the lamination thickness down to about 0.00033 in. This would require the use of a toroidal tape-wound core, the suggested winding arrangement having the primary as a distributed winding round the circumference of the toroid with the secondary in a tall and narrow section at one place. Since nearly all the outside of the secondary would then be in open space, secondary stray capacity could probably be reduced, with care, to about 15 pF. With thinner magnetic material, the turns required for equalizing the noise contributions from the shunt and series losses would be less than with thicker material, and difficulty might be experienced in keeping the primary inductance sufficiently high. A material such as Supermalloy could be used if necessary, however, the very high permeability of which should overcome the difficulty.

In aiming to obtain the very best possible noise factor, it would be best to limit the working frequency range to that applying when the tuned circuit is in use, rather than try to achieve an alternative wide bandwidth in the same design, as done in the present equipment. In designing for optimum performance at frequencies well under 800 c/s, it would be necessary to consider flicker noise, which would result in the optimum valve current being lower than the optimum for higher frequencies.

It will be seen from Figure 14 that the valve current used in the equipment described in the present paper is considerably less than the optimum for 800 c/s operation, which would be in the region of 1 mA. It will be noticed, however, that the increase in noise is very gradual for a reduction of valve current below the optimum, but much more rapid above the optimum; it is desirable in practice, therefore, to operate at, say, about half the true optimum current, so that a slight increase in grid current will not cause too great a deterioration in performance.

6. REFERENCES

(1) Moxon, L.A.: Recent Advances in Radio Receivers (Cambridge University Press).

(2) Gillespie, A.B.: Signal, Noise and Resolution in Nuclear Counter Amplifiers (Pergamon Press).

(3) Baxandall, P.J.: "Hum in High-Gain Amplifiers", Wireless World, February 1947.

(4) Cooper, W.H.B., Seymour, R.A., and Walker, D.C.: "The Behaviour of Ferromagnetic Materials at Low Flux Densities", Post Office Research Report No. 12258.

(5) Story, J.G.: "Design of Audio-Frequency Input and Inter-Valve Transformers," Wireless Engineer, February 1938.

(6) Couzens, E.G., and Wearmouth, W.G.: "Plastics in the Radio Industry", Electronic Engineering Technical Monograph.

(7) Nottingham, Prof. W.B.: "Electrometer Tube Development", M.I.T. Electronics Research Lab. Final Report, June 30, 1946.

(8) Bayard, R.T., and Alpert, D.: "Extension of the Low Pressure Range of the Ionization Gauge", Rev. Sci. Instrum., 21, p.571 (1950).

APPENDIX 1

(a) Effect of Shunt Resistance on Noise Factor

The Noise Factor of any device may be defined in several ways, but the simplest definition for the present purpose is:-

$$\text{Noise factor in decibels} = 10\log_{10} \frac{\text{Total mean square noise output voltage}}{\text{Component of mean square noise output voltage due to Johnson noise in input source impedance}}$$

Referring to Figure A, let the signal source have resistance R_o at temperature T_o, being shunted by a resistance R_{sh} at temperature T_{sh}. Then the noise factor is given by:-

$$N.F. = 10\log_{10} \frac{\left[(4kT_oR_o\delta f)^{\frac{1}{2}} \times \frac{R_{sh}}{R_o + R_{sh}}\right]^2 + \left[(4kT_{sh}R_{sh}\delta f)^{\frac{1}{2}} \times \frac{R_o}{R_o + R_{sh}}\right]^2}{\left[(4kT_oR_o\delta f)^{\frac{1}{2}} \times \frac{R_{sh}}{R_o + R_{sh}}\right]^2}$$

$$= 10\log_{10} \frac{T_o R_o R_{sh}^2 + T_{sh} R_{sh} R_o^2}{T_o R_o R_{sh}^2}$$

$$= 10\log_{10} \left[1 + \frac{T_{sh} R_o}{T_o R_{sh}}\right] \text{ dB} \qquad \ldots (i)$$

The second term in the brackets may be regarded as the undesired contribution due to the shunt loss resistance R_{sh}, the first term being the desired contribution due to Johnson noise in the source.

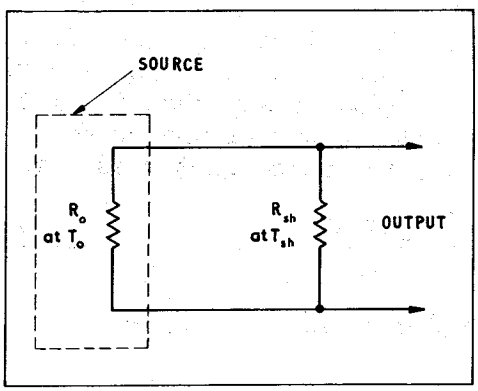

Figure A

(b) Effect of Series Resistance on Noise Factor

Referring to Figure B, let the signal source have resistance R_o at temperature T_o, having in series with it a resistance r_{se} at temperature T_{se}. Then the noise factor is given by:-

$$N.F. = 10\log_{10} \frac{4kT_oR_o\delta f + 4kT_{se}r_{se}\delta f}{4kT_oR_o\delta f} \quad \ldots \text{(ii)}$$

$$= 10\log_{10} \left[1 + \frac{T_{se}r_{se}}{T_oR_o}\right]$$

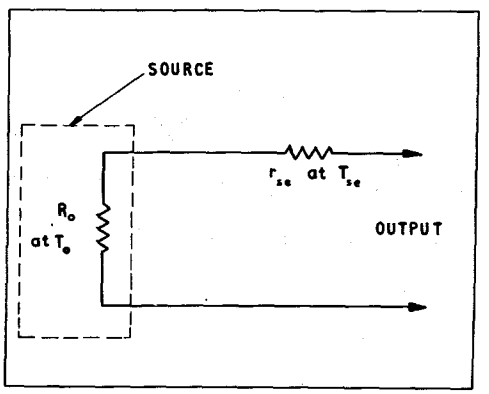

Figure B

(c) Effect of Combined Shunt and Series Resistance on Noise Factor

When both shunt and series resistances are simultaneously present, the noise factor may be calculated in the same basic manner as above, but the result depends on the position of the series resistance in relation to the shunt resistance. However, on the assumption that R_{sh} is much greater than R_o and r_{se} much less than R_o - a condition which applies in the present design problem - the relative position of the resistances is of negligible importance, and it is approximately true to say that the noise contributed by one resistance is independent of the presence of the other. Under these conditions, the noise factor is given by:-

$$N.F. = 10\log_{10} \left[1 + \frac{T_{sh}R_o}{T_oR_{sh}} + \frac{T_{se}r_{se}}{T_oR_o}\right] \quad \ldots \text{(iii)}$$

If $T_{sh} = T_{se} = T$, then the noise factor is given by:-

$$N.F. = 10\log_{10} \left[1 + \frac{T}{T_o}\left(\frac{R_o}{R_{sh}} + \frac{r_{se}}{R_o}\right)\right] \quad \ldots \text{(iv)}$$

APPENDIX 2

The following calculation refers to the condition when a 300 ohm source, at 20°K, is connected directly to the room-temperature transformer. The calculated transformer loss resistance values are used, but the equivalent valve noise resistance is the measured value of 25 kilohms.

Source resistance referred to grid

$= 300 \times (59.6)^2 \times 10^{-6} = 1.07$ megohms. Mean square noise ... 1 UNIT

Copper resistance of room-temperature transformer, referred to grid

$= 4.0 + 1.30 \times (59.6)^2 = 8.62$ kilohms

Hence, from Appendix 1, relative noise contribution from this loss
$= (290/20) \times (0.00862/1.07)$
$= 0.117$ Unit. Mean square noise ... 0.117 UNIT

Eddy-current loss of room-temperature transformer, referred to grid, 72megohms

Hence, from Appendix 1, relative noise contribution from this loss
$= (290/20) \times (1.07/72) = 0.216$ Unit Mean square noise ... 0.216 UNI

Relative noise contribution from shot and partition noise
$= (290/20) \times (0.025/1.07)$
$= 0.339$ Unit Mean square noise ... 0.339 UNI

From formula (19) of Section 5.4, assuming a grid current of 10^{-11}A, which is the maximum value quoted by the makers for the conditions used, the relative contribution from grid-current noise = 0.003 Unit . Mean square noise ... 0.003 UNI

.. TOTAL mean square noise, other than from source ... 0.675 UNI

Hence Noise Factor = $10\log_{10}(1 + 0.675) = 2.24$ dB

(With a shunt loss resistance of 36 megohms, as obtained by measurement in room-temperature transformer No. 1, the relative noise contribution from this cause is 0.432 Unit, giving a Noise Factor, with the other contributions as above, of 2.77 dB, which agrees well with the measured Noise Factor).

SOME ASPECTS OF SOLAR RADIO NOISE

By V. A. Hughes, M.Sc., F.R.A.S.

The dramatic discovery by J. S. Hey[1] in 1942 that sunspots were capable of emitting intense radiation at metre wavelengths was not made public until the lifting of security restrictions in 1946. Since then a great deal of information has been obtained both in this country and abroad on the behaviour of solar radio wave radiation in the band which is limited at longer wavelengths by attenuation in the ionosphere and at shorter wavelengths by atmospheric absorption and receiver sensitivity. Various types of radiation are now recognised, and it is possible to detect not only the intense levels related to solar activity but also the basic thermal radiation and to confirm the results suggested by optical methods that the temperature in the solar corona is of the order of 10^6 deg.K.

It is not the purpose here to give a complete survey of solar radiation but to give a general picture and to deal with some of the more recent work. It is convenient to classify solar radiation into three components[2]; the background level of the quiescent sun, the slowly varying component associated with sunspots and the more rapid short duration increases normally associated with solar flares. These three divisions, known as the B, S and X components respectively, will be considered in turn. Finally a description will be given of some of the measurements made at R.R.E. during the solar eclipse of 30th June, 1954.

The Background Radiation (B Component)

At optical wavelengths the sun appears as a bright disk, surrounded by a faint atmosphere or corona. Because of the great contrast between the corona and the sun itself it is normally only seen at times of a total eclipse. Its form at the time of the total eclipse of 30th June 1954 is shown in Plate I. This corona consists mainly of ionized hydrogen which, though transparent to optical wavelengths, absorbs and emits radiation at radio wavelengths to a degree depending on electron density and temperature. Most of the radiation at a particular wavelength will originate close to the region in the corona where the absorption is high, and the radiation received will approximate to that corresponding to the electron temperature at that point. Also, the limit to propagation of radiation is that the refractive index must be greater than zero. Since the refractive index becomes zero at the wavelength λ where $\lambda^2 = K/N$, K being a constant and N the electron density, and since the electron density increases with decreasing height in the corona, the shorter the wavelength the greater the depth from which radiation may be received. This is shown in Figure 1, for the case where there is no magnetic field. However, the electron temperature increases with increasing radial distance from the sun, rising from about 6000 deg. K at the photosphere to about 10^6 deg. K in the corona, and since the intensity received along a ray path originating in the sun is

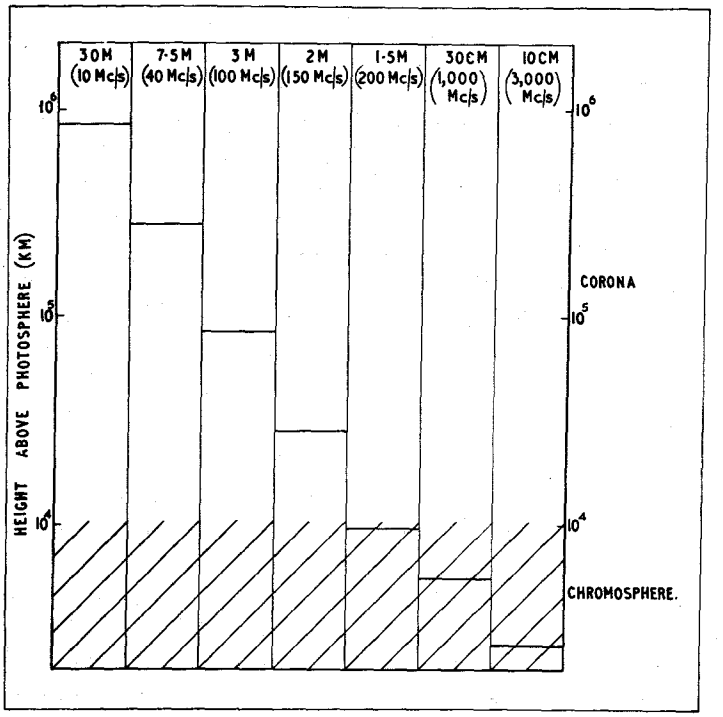

Figure 1

Lowest Level in Solar Atmosphere from which Radiation can escape, assuming no Magnetic Field

a function of the absorption (proportional to N^2), the refractive index and the electron temperature along that path, the intensity distribution across the sun may be expected to be non-uniform. A ray originating towards the limb will travel a greater distance in the higher temperature corona than a ray which originates from the centre of the disk, and refraction of the rays in traversing regions of the corona where the refractive index departs from unity will also modify the distribution.

It was first suggested by Martyn[3] that, though at wavelengths of the order of 1 metre the solar radio disk would tend to be uniformly bright and at a temperature of about 10^6 deg. K. corresponding to the coronal temperature, at wavelengths of 60 cm and less the radiation from the centre of the sun would decrease since it originates mainly in the lower temperature corona and chromosphere, whilst the radiation from the limb would not decrease as rapidly due to the rays traversing the higher temperature corona. The result

would be that the sun appears to have a bright ring round the limb. Similar calculations have been made by others including Hagen [4] and Smerd [5] using modified electron temperature distributions and taking into account the effect of refraction in the corona. The results all indicate "limb brightening" at the shorter wavelengths, the wavelength at which it occurs and its amplitude depending on the assumed parameters of the coronal model.

Difficulty arises over the testing of the various coronal models. A high resolving power is required and measurements may be distorted by the presence of high intensity sources on the solar disk. Three methods have been used; interferometer methods, the use of large aerials and eclipse measurements.

Interferometer methods. The principle of this method is analogous to the Michelson interferometer. A series of measurements are obtained by using two aerials at various spacings. At each spacing the amplitude of the signal obtained when the source passes through the interference lobes of the two aerials is proportional to the angular frequency component corresponding to the lobe spacing across the source, and the distribution across the source is given by the Fourier transform of the curve relating signal amplitude to aerial spacing. Stanier [6] used this method at a wavelength of 60 cm but failed to detect any evidence of limb brightening, but more recent measurements by O'Brien and Tandberg-Hanssen [7] using interferometers with axes inclined at various angles to the solar axis of rotation have shown that not only is there limb brightening but the limb brightening is confined to the equatorial regions, the maximum occurring at 0.6 R_o and not at 1.0 R_o as predicted from theory. (R_o is the radius of the photosphere). This lack of agreement may be due to either a change in electron density during the sunspot cycle as has been shown from a recent analysis by Van de Hulst [8] or to the presence of emitting regions on the sun at the time that Stanier was obtaining his measurements. That the sun should show some form of non-radial symmetry is not surprising from examination of photographs of the solar corona and this has been confirmed by O'Brien [9] at the wavelength of 1.4 metres, this result also showing limb brightening at the equator. Some contours of radio noise across the solar disk obtained using interferometer techniques are shown in Figure 2.

Large aerial systems. To obtain an angular resolution corresponding to 1/10th the solar subtension, a beamwidth of 3 mins. of arc is required. This implies an aerial aperture of just over 1000 wavelengths. Such large aerials involve difficulties because of their size at metre wavelengths and tolerances in construction at short wavelengths. However, a large 50 ft. diameter paraboloid which can be used at wavelengths down to about 8 mm has recently been constructed at the Naval Research Laboratories, Washington, and results as yet unpublished suggest that at this wavelength both centre and limb brightening exist.

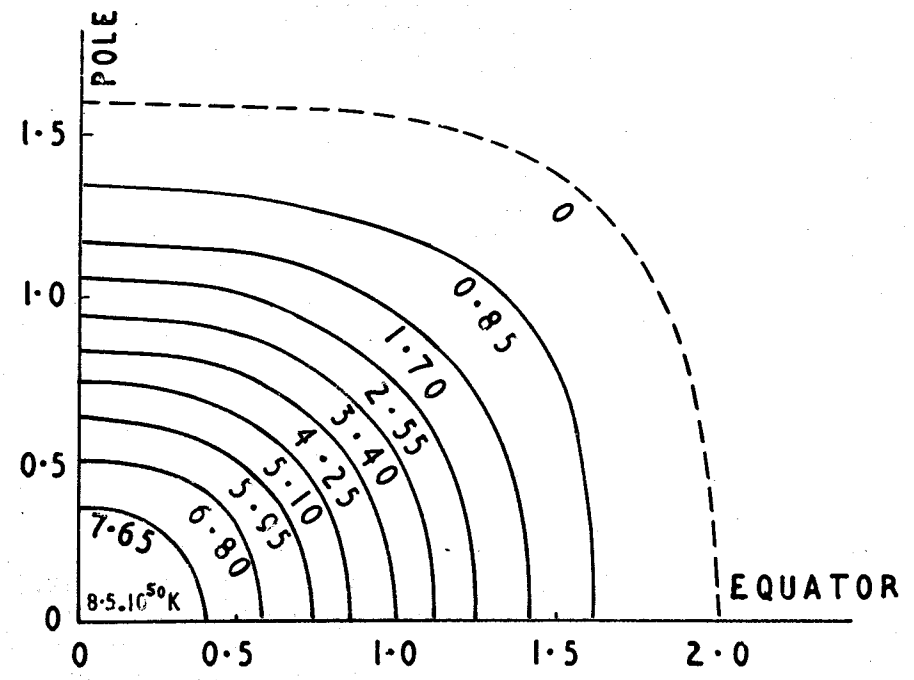

FIGURE 2 (a)

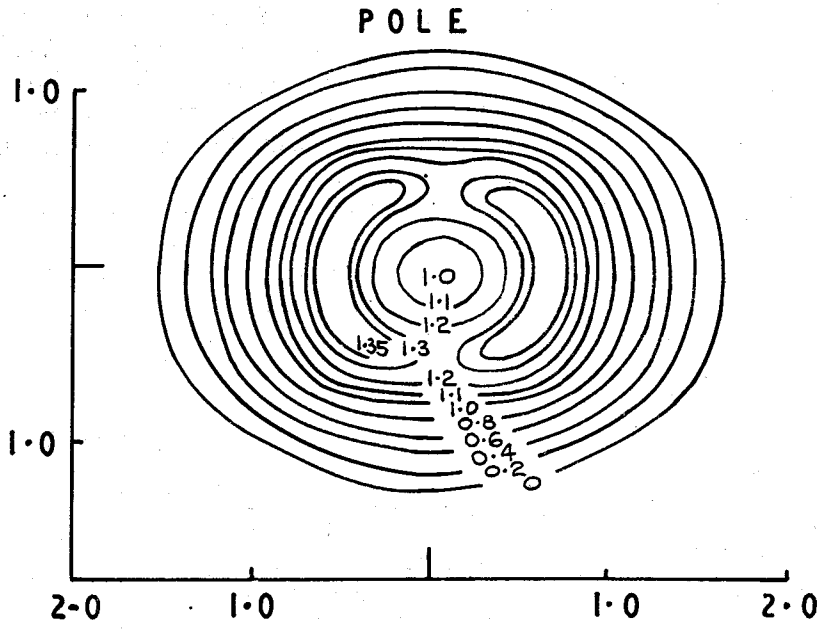

FIGURE 2 (b)

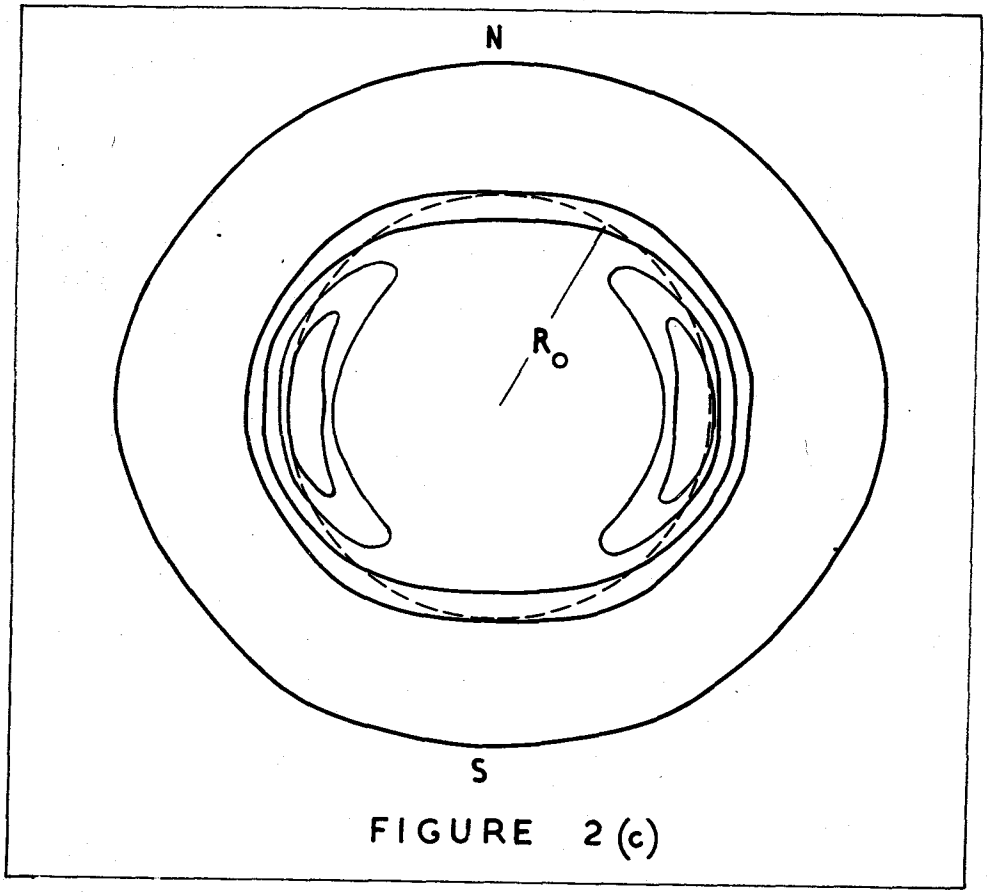

FIGURE 2 (c)

Figure 2

Distribution of Radio Brightness
across the Sun, with Radius of Photosphere as Unit

(a) λ = 1.4 m. Interferometer technique (O'Brien)
(b) λ = 60 cm. Interferometer technique (O'Brien & Tandberg-Hanssen)
(c) λ = 21 cm. Diffraction grating (Christiansen & Warburton).

It is easier to obtain a discrimination in one dimension by the use of a linear array and some aerials of this type have been constructed. Covington and Broten[10] use a waveguide array 150 ft. long, giving a beamwidth of 8 mins. of arc and, by use of a linear diffraction grating consisting of 32 paraboloids, Christiansen[11] has obtained a resolution of 3 mins. of arc at the wavelength of 25 cm and Swarup and Parthasarathy[12] 8.26 mins. of arc for the wavelength of 60 cm using the same apparatus.

All these experiments show a brightening towards the limb in the one dimensional case. The use of the diffraction grating in two orthogonal planes [13] also shows a lack of circular symmetry, Figure 2.

Eclipse results. The main advantage of eclipse measurements is the increased resolving power, especially for the measurement of bright sources, but the accuracies obtained for the radial distribution are not very high. They do provide a means of checking results obtained by other methods and originally led Denisse, Blum and Steinberg [14] to conclude that at a wavelength of 1.8 metres the sun showed marked departures from radial symmetry. This result was arrived at from measurements taken at three widely separated points, one on the path of totality and two others at sites where the eclipse was partial. The path of the moon's centre across the sun and the shape of the radio sun is shown in Figure 3. Recent measurements made by Hey and Hughes [15] during the eclipse of 30th June, 1954 indicate that at a wavelength of 10.5 cm a small amount of asymmetry exists; this will be described later in more detail, and Steinberg (private communication) suggests that even at 3 cm non-radial symmetry exists.

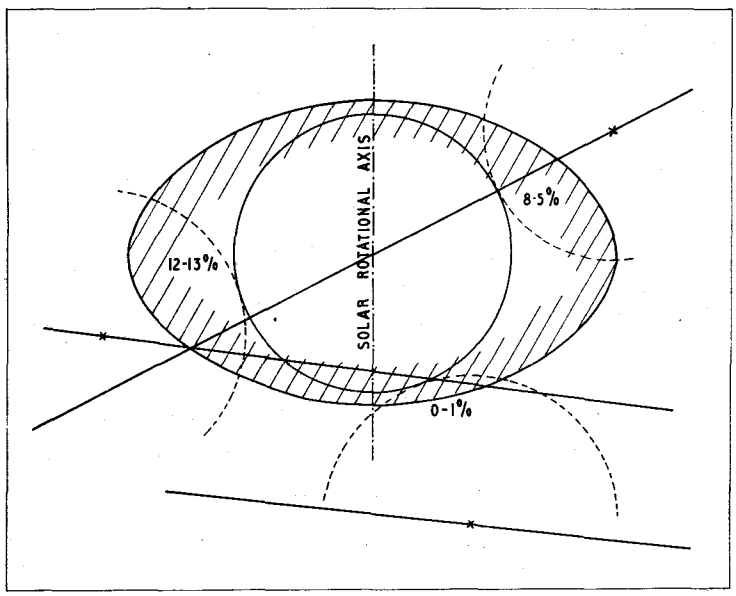

Figure 3

The Shape of the Radio Sun at $\lambda = 1.78$ m., obtained from the Solar Eclipses of 1st Sept. 1951 and 25th Feb. 1952

The straight lines indicate the locus of the moon's centre and the percentages shown are the reduction in solar intensity at the optical contacts (Denisse, Blum & Steinberg).

Discrepancies exist in the measurements made by the different methods and by the same methods used at different times. It is possible that the background level may vary and that the shape of the radio sun may change in form, as does the shape of the solar corona, depending on the phase of the sunspot cycle. The presence of bright radio sources on the sun, even in the absence of sunspots, may also lead to some of the discrepancies. However, Piddington[16] has analysed the available information and obtained curves showing the apparent disk temperature and central brightness temperature for the average spot free sun (ca 1948) and for the sun after a prolonged absence of sunspots. This is shown in Figure 4.

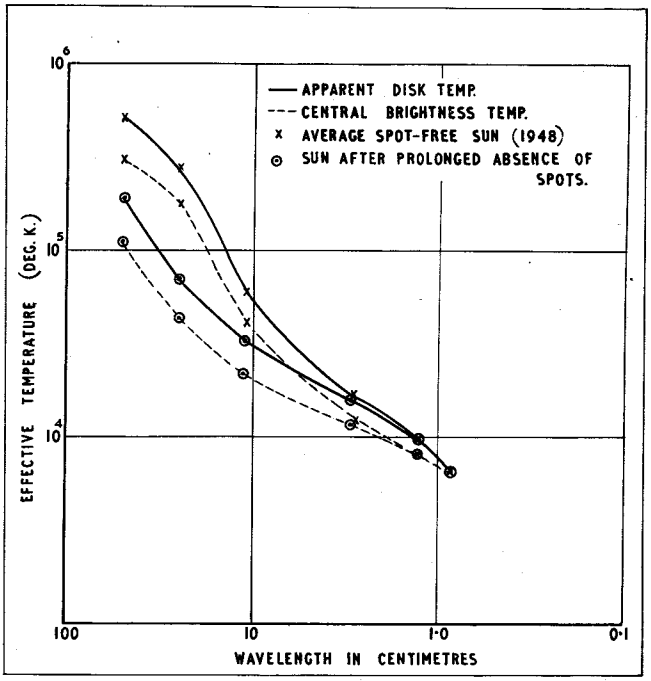

Figure 4

Curves of Solar Temperature (B Component) against Wavelength (Piddington)

The Slowly Varying Component (S Component)

During radio observations of the eclipse of 23rd November, 1946 at a wavelength of 10.3 cm, Covington[17] noticed, from the obscuration of a sunspot group, that the signal received from the sunspot was very much greater than that from the remainder of the disk. That sunspots are the source of increased radiation has also been shown in a similar manner by other workers [18, 19, 20] at wavelengths of 50 cm, 10 cm and 3.2 cm. Covington also showed[21] that the variations in 10.7 cm radiation from the sun showed striking similarity to the variations in sunspot number, and Denisse[22] taking the analysis further found successively better correlation between increased solar radiation and sunspot number (N), integrated sunspot area (ΣA) and the factor $\Sigma A \frac{H_o}{\sqrt{A}}$ where H_o is the

magnetic field of the sunspot. Piddington and Minnett[2] have used the results of other workers [23, 24, 25] together with Covington and their own to obtain the spectrum of the S component in terms of increased solar temperature per unit sunspot area. Their results are shown in Figure 5. Most of the radiation is circularly polarised.

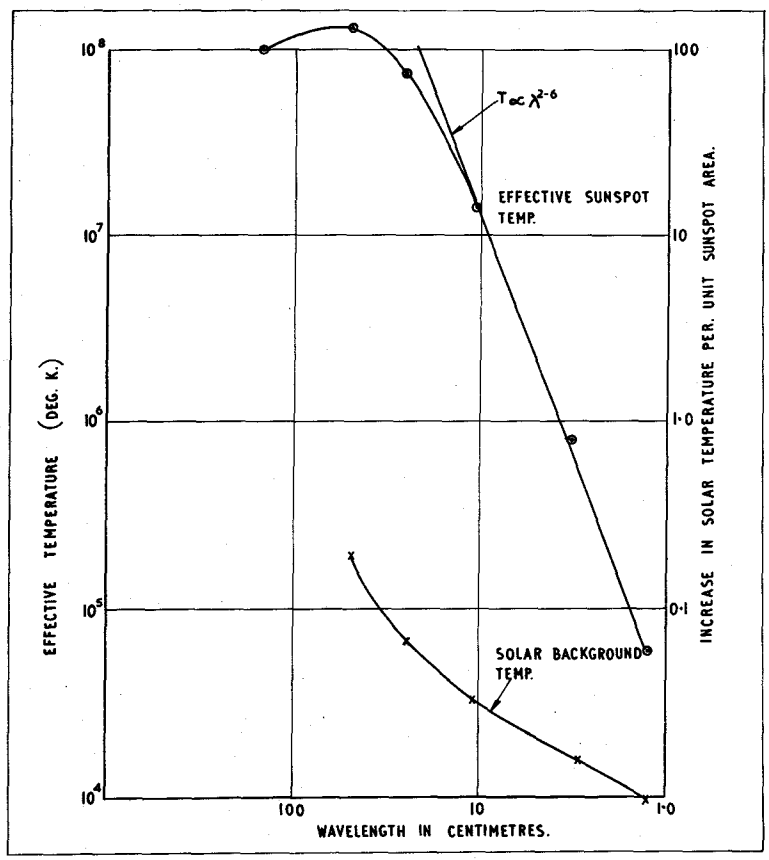

Figure 5

Spectra of Sunspot & Background Radiation against Wavelength

The unit of sunspot area is 10^{-6} x solar area.

If the emitting area is the same as the sunspot area, it is possible to determine the effective temperature of sunspots and, using this assumption, Figure 5 also shows the effective sunspot temperature in comparison with the effective temperature of the spot-free sun. There is not precise agreement between the temperatures obtained by this means and those obtained by Covington and

Broten[10] using the 150 ft. waveguide array, results from the latter, for three sunspots, varying from 3.10^5 to 2.10^6 deg. K as against 10^7 deg. K. This may be explained by the fact that Covington and Broten take the emitting region as being larger than the sunspot area, whereas the other method is a statistical one and may be influenced by the presence of bright regions not associated with visual spots.

The slowly varying component does not involve temperatures greatly in excess of coronal temperatures and, since there are no a priori arguments to decide between thermal and non-thermal mechanisms, the simplest hypothesis is that it originates in coronal condensation above the level of a spot. If the coronal density were to increase, the temperature distribution remaining constant, then radiation at a particular frequency would originate at greater heights in the higher temperature regions, and an increase in diameter of the emitting region of ten times over the diameter of the spot at a region in the corona where the temperature is 10^6 deg.K would show the sunspot as having an effective temperature of 10^8 deg. K, in agreement with the curve of sunspot temperature as shown in Figure 5. A model of a coronal condensation as suggested by Waldmeier and Muller[26] is shown in Figure 6.

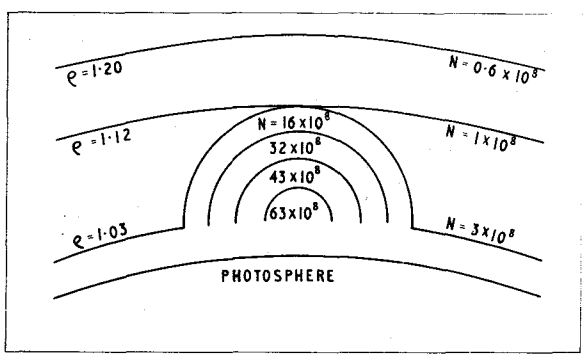

Figure 6

Model Coronal Condensation

The diameter is 125,000 km. Electron densities, N, are per c.c. (Waldmeier & Muller)

That noise storms originate in high regions in the solar atmosphere has been shown by Payne-Scott and Little[27], who measured sources at heights of 0.3 to 1.0 photospheric radii above the sun's visible surface, using a wavelength of 3.1 metres. Though noise storms are, strictly speaking, not the slowly varying component, they are the manifestation of sunspot radiation at longer wavelengths, and usually occur when sunspots are on the centre of the disk. In other words, though at centimetre wavelengths the radiation from sunspots tends to be isotropic, producing the true slowly varying component, at longer wavelengths they have directional characteristics, producing noise storms, and Machin and O'Brien[28] have shown that the emission widths, between half power points, are 36°, 20° and 15° for wavelengths of 50 cm, 1.7 metres and 3.7 metres respectively, these angular widths corresponding to increases lasting for 2.7, 1.5 and 0.6 days respectively.

Burst (X Component)

The X component consists of increases in radio noise of short duration, usually associated with solar flares or small brightenings on the solar disk observed in the $H\alpha$ spectral line from atomic hydrogen. Flares, besides producing radio effects, are also thought to be a source of cosmic rays, X-rays and ultra violet radiation, as well as being involved in the emission of corpuscular streams, all of which cause terrestrial effects such as ionospheric disturbances, magnetic storms and aurorae.

At the wavelength of 10.7 cm, the X component consists mainly of increases in radio noise of up to the order of a few times the basic component and has been classified by Dodson, Hedeman and Covington[29] into six categories; these include simple bursts, multiple bursts, gradual rise and falls, and combinations of these. It is found that if a flare occurs on the solar disk there is a 57% probability of a radio burst, independent of the position of the flare, whilst gradual rise and falls result more frequently when a flare is on the centre of the disk, and last as long as or longer than the flare. In either case, a radio event appears always to be associated with a flare. Figure 7 shows an unpublished result obtained by Hey and Hughes of the variation in solar radiation with the line widths of $H\alpha$ during an intense flare of 18th May 1951. The $H\alpha$ variation was kindly supplied by Ellison from the Royal Observatory, Edinburgh.

At metre wavelengths the X component becomes more intense and, using the panoramic receiver, Wild[30] has obtained spectra of the so called "outbursts" in the range of 70 - 130 Mc/s showing a drift in spectral features towards low frequencies at a rate of about 1/4 Mc/s per sec. The extension of the range to 40 - 210 Mc/s[31] shows an initial very rapid drift together with the

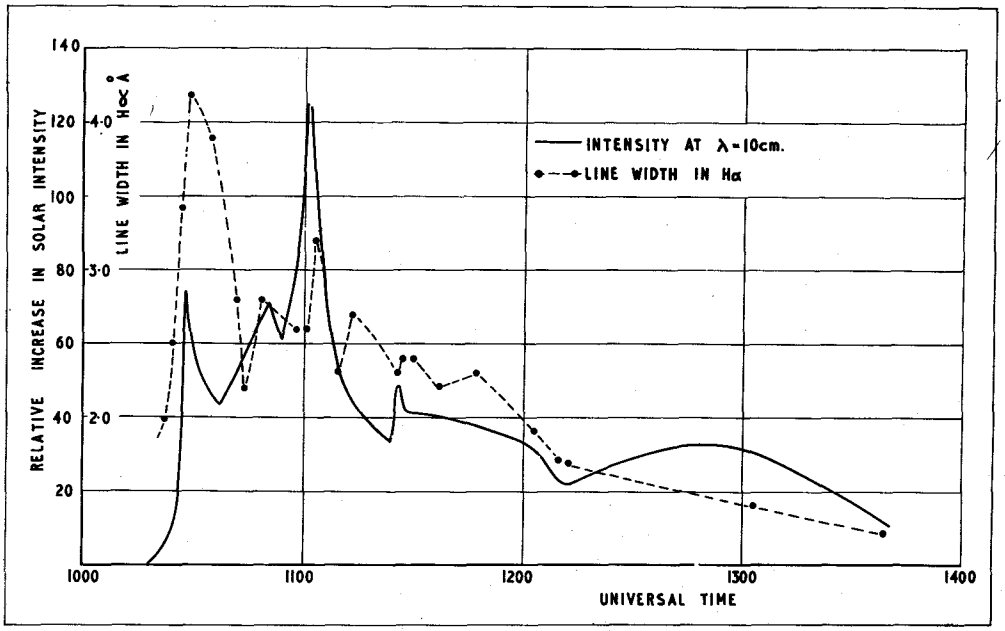

Figure 7

Comparison between Increased Solar Radiation at λ = 10 cm. and Line Width of Hα during Solar Flare of 18th May, 1951

previously measured slow drift with the addition of a second harmonic term, the latter being shown in Figure 8. The interpretation of these results is based on the principle that radiations at a particular wavelength can only escape from the sun when the source reaches a height where the electron density is such that the refractive index is greater than zero; the flare initiates firstly a component of high velocity - about a third that of light - which may be associated with cosmic rays, followed by the much slower component with velocity of about 400 - 600 km/s which appears to be associated with the emission of corpuscular streams. Whatever the cause of the intense radio emission, it appears that some non-linear mechanism is operative and the radiation is non-thermal.

Further confirmation of the movement of sources of intense radiation on the solar disk was obtained by Little and Payne-Scott[32]. In this case, the movement of the sources in directions across the disk normal to the line of sight was observed by means of an interferometer, the lobes being swept across the sun 25 times a second. Six outbursts

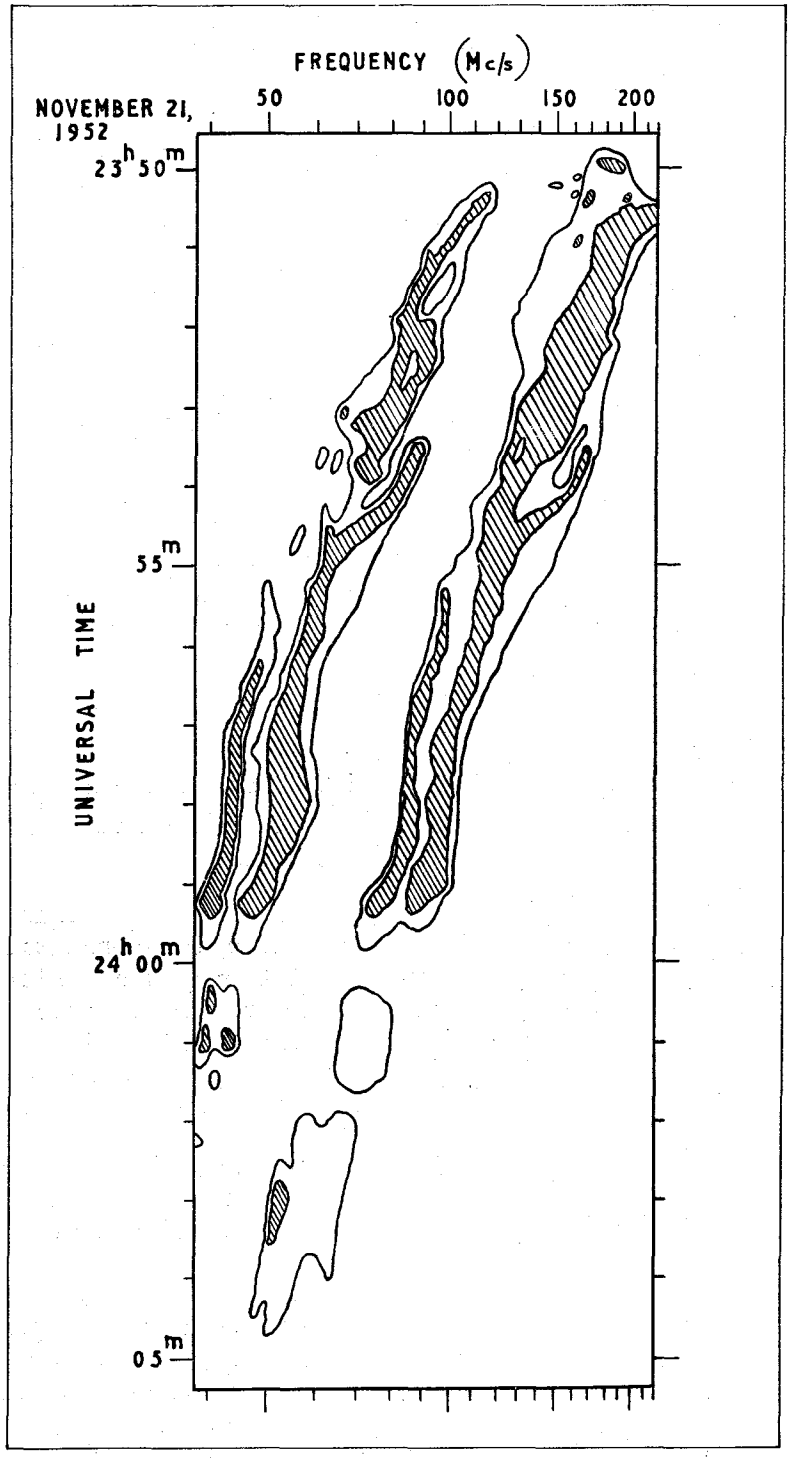

Figure 8

The Dynamic Spectrum of an Outburst (21st Nov. 1952), showing Second Harmonic Term (Wild, Murray and Rowe)

were observed, initiated by flares, and in each case large scale movements were observed together with changes in polarization. Initially, the polarization was random, but during the course of the flares the radiation appears to go through stages of circular, linear or elliptical and finally circular polarization.

An interesting feature of radio bursts was first pointed out by Hey, Parsons and Phillips[33] who reported that, at a wavelength of 4.1 metres, radio bursts associated with solar flares occurred more often on the eastern half of the sun than on the western. The explanation of this was that the region of the flare is the source of corpuscular emission which, because of solar rotation east to west, sprays out like a rotating hosepipe. Hence a flare on the west of the sun will be more obscured than one on the east. A more recent analysis at the shorter wavelength of 1.5 metres by Dodson, Hedeman and Owren[34] failed to indicate any significant asymmetry but, as pointed out by Hey and Hughes,[35] this may be due to the expected smaller absorption at the shorter wavelength and far more results would be required to obtain a significant answer. Further analysis by Hey and Hughes[36] confirms the asymmetry and it is pointed out that absorption, if absorption is the cause, must be taking place close to the source of radiation. This kind of analysis is important since, though corpuscular streams are assumed to exist and go a long way to explain a number of terrestrial effects such as magnetic storms and aurorae, very little direct evidence of their existence has been obtained.

Solar Eclipse Measurements of 30th June 1954

A solar eclipse is of interest to radio astronomers since it enables check measurements to be made on the form of the distribution across the sun. The eclipse of 30th June 1954 was ideal since it occurred at a time of sunspot minimum, at a time when there appeared to be no disturbed regions on the solar surface. The path of totality stretched from the centre of the North American Continent, through Southern Greenland and Scandinavia to the borders of India, the centre of the path being in South Scandinavia.

Two expeditions were organised from R.R.E., one to the path of totality in Southern Norway where measurements were made at a wavelength of about 8 mm, and one to a local site near Malvern where measurements were obtained at the two wavelength bands of 3 cm and 10 cm. In order to give some idea of the type of equipment used and the results obtained, only the 10 cm measurements will be described.

The object of the experiment was to determine the shape of the sun at the wavelength of 10 cm, with a view to measuring the extent of limb brightening, by observing the way in which the intensity of the received radiation from the sun varied throughout the eclipse. If it may be assumed, as is possibly true at the very short microwavelengths, that the distribution across the sun shows circular symmetry, then the maximum

amount of information is obtained in a region where the eclipse is total. But, since for totality the path of the moon's centre is along a solar diameter, the eclipse curve will be symmetrical with respect to sun-moon separation irrespective of whether the radiation is circularly symmetrical or tends towards the type of distribution as in Figures 2 or 3, and a large number of solutions will be found to fit the experimental results. On the other hand, if observations are taken where the eclipse is partial, the path of the moon's centre follows a chord on the solar surface; if the eclipse curve is symmetrical then it is justified to assume circular symmetry, whilst if the two halves of the eclipse curve are not the same, added information is obtained concerning the shape of the distribution which may suggest further experiments. The Malvern area was ideal for checking solar symmetry, since at totality about three quarters of the sun was eclipsed.

Owing to the small power levels involved, it was necessary to choose a site that was free from interference, and with this in mind it was decided to set up the equipment in Ledbury, about 7 miles from Malvern, and screened from the radar interference of the Establishment by the line of the Malvern Hills. The equipment was positioned and set in operation about a week before the day of the eclipse.

The Radiometer

The radiometer is an equipment designed to measure small noise powers normally with an accuracy corresponding to variations in effective temperature of 1 deg. K. At microwavelengths these measurements are made with receivers having internal noise levels corresponding to an input noise power of about 3000 deg.K, and if a simple "straight" receiver were used a high degree of gain stability would be required. This difficulty was partially overcome by Dicke[37] who reduced the effect of receiver gain variations by periodically inserting a disk of attenuating material into the waveguide between the aerial and the receiver, using the receiver to measure the difference between the aerial temperature and the temperature of the disk. The difficulty still remains of measuring accurately aerial temperatures near absolute zero or room temperature, since in the former case a gain stability of the order of 0.3% is required, and in the latter case difficulty arises in the accurate measurement of the temperature of the rotating attenuator disk.

The present system overcomes the remaining difficulties by the use of a waveguide switch which alternately switches the receiver, about 30 times a second, between the aerial and a standard noise source consisting of a variable precision attenuator and accurately

calibrated argon discharge tube [38] and, since the aerial temperature is liable to be less than room temperature, a directional coupler is used to increase the effective temperature of the aerial arm of the switch by about 300 deg.K. The receiver is used as a null detector or a vernier enabling small temperature variations about the value corresponding to the setting of the attenuator of the standard noise source to be measured.

The block schematic diagram of the radiometer is shown in Figure 9, the remainder of the equipment following conventional lines. The gain of the receiver was such that full scale deflection of the recorder corresponded to about 10% of the total received solar noise; as the eclipse progressed, the standard noise source was reset in order to keep the recorder on scale. The resulting relative accuracy in measurement of the eclipse curve corresponded to 1 deg. K or 0.5% of the level of the uneclipsed sun.

The aerial or radio telescope consisted of a 5 ft. diameter paraboloid mounted on the roof of a radar cabin. To enable the aerial to follow the sun, azimuth and elevation information was fed into the servo-controls from a computer. The computer[39] is based on a model of the celestial sphere, and is shown in Plate II.

The calibration of the whole equipment was obtained by directing the aerial towards a waveguide horn fed from a discharge tube. The waveguide horn simulates a source whose area is given by the effective area of the horn and whose temperature is the same as the effective temperature of the discharge tube (11,190 deg.K). By measuring the increase in effective temperature of the aerial, and knowing the effective angular subtension at the aerial of the waveguide horn, the calibration is obtained.

The Results

The sky was cloudy on the morning of the eclipse, but there were sufficient clear patches to allow last minute optical checks on the alignment of the aerial. As the eclipse progressed the sky became completely overcast, but it was reassuring to note that at the end of the eclipse the solar level had returned to its pre-eclipse value. In order to check the alignment accuracy of the aerial, measurements were repeated the following day, and it was confirmed that the aerial was positioned accurately on the sun throughout the region of the sky covered by the eclipse.

The eclipse curve obtained is shown in Figure 10 together with the path of the moon's centre across the sun. The initial feature observed from the curve is the slight asymmetry in the two halves, this asymmetry appearing more obvious when the two halves of the curve are plotted in terms of the sun-moon separation as in Figure 11. The probable explanation of this is that the distribution across the sun is not circularly symmetrical, but tends more to an elliptical shape. This is also suggested

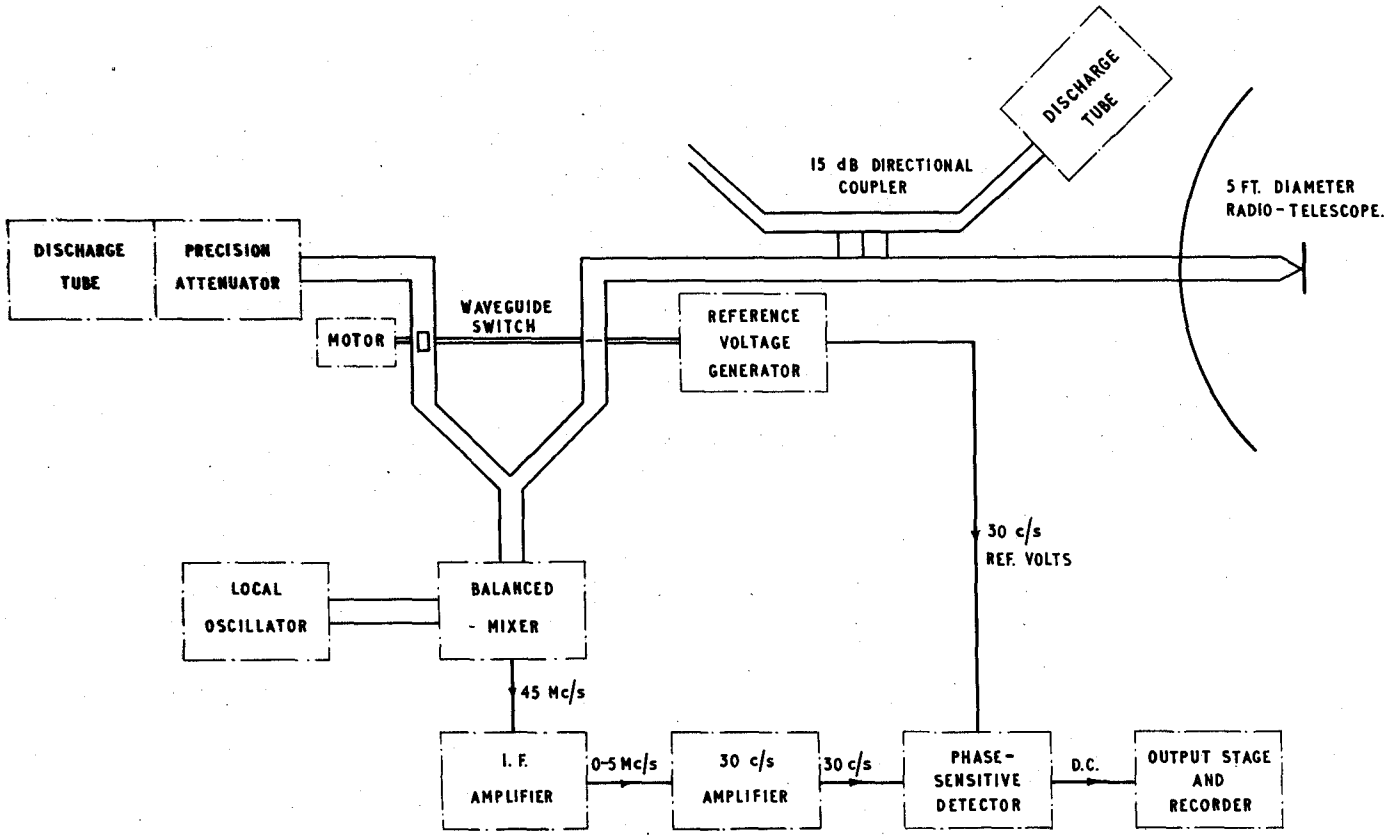

FIGURE 9.

SIMPLE BLOCK SCHEMATIC DIAGRAM OF RADIOMETER.

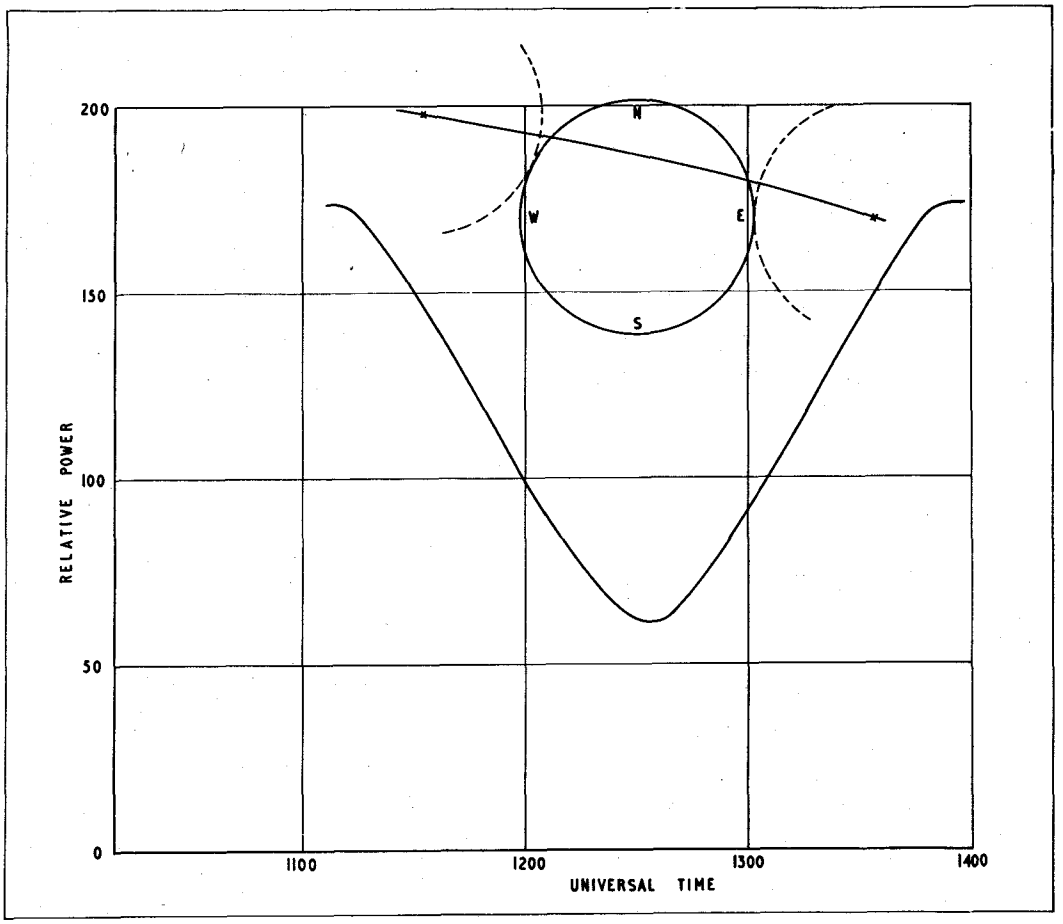

Figure 10

Eclipse Curve for 30th June, 1954,
together with Path of the Moon's Centre
with respect to the Solar Disk

by the fact that the radius of the sun is slightly greater at the end of the eclipse than at the beginning. A comparison of the eclipse curve with the curve that would have been obtained had the sun uniform brightness shows that the decrease at the start of the eclipse is more rapid and hence indicates a greater intensity at the limb than for a uniform model. This also holds if a uniform disk is assumed of radius 10% greater than the optical disk, this figure being the suggested value for the size of the radio disk from timing the start of the radio eclipse. Hence the results obtained indicate that, at the wavelength of 10 cm, the form of the sun is probably somewhat similar to that at slightly longer wavelengths (cf. Figure 2). It is interesting to note that, even at the wavelength of

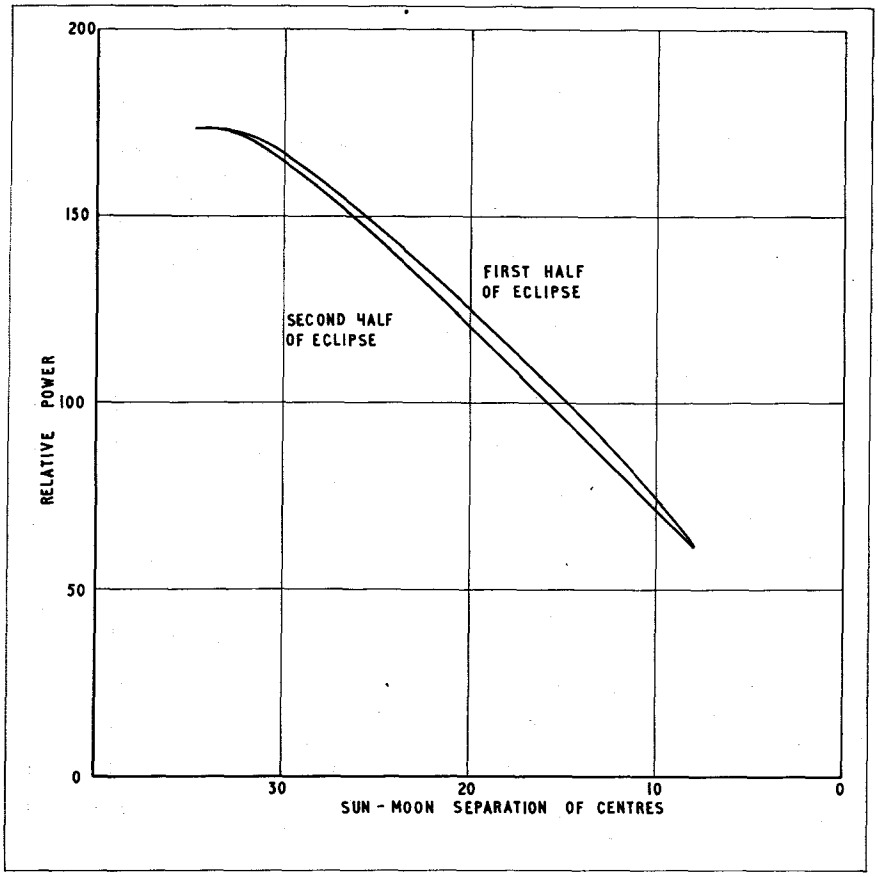

Figure 11

Comparison of Two Halves of

Eclipse Curve

3 cm, Steinberg (private communication) suggests that the asymmetry still exists.

A more detailed analysis is at present in progress; the initial results suggest a certain amount of limb brightening.

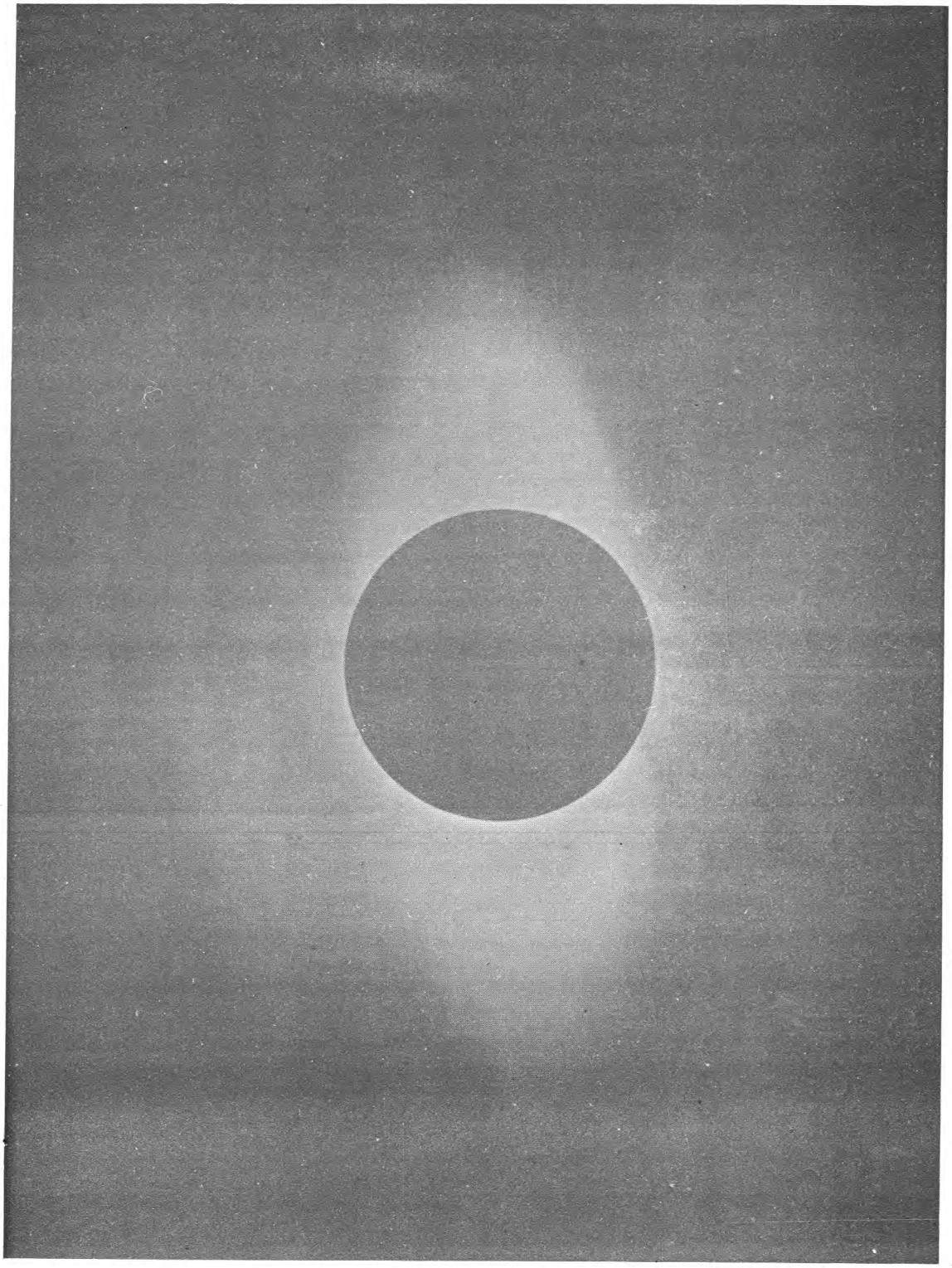

PLATE I The Solar Corona, 30th June, 1954, photographed by the Royal Greenwich Observatory expedition to Sweden and reproduced by permission of the Astronomer Royal. The photograph was taken through thin cloud.

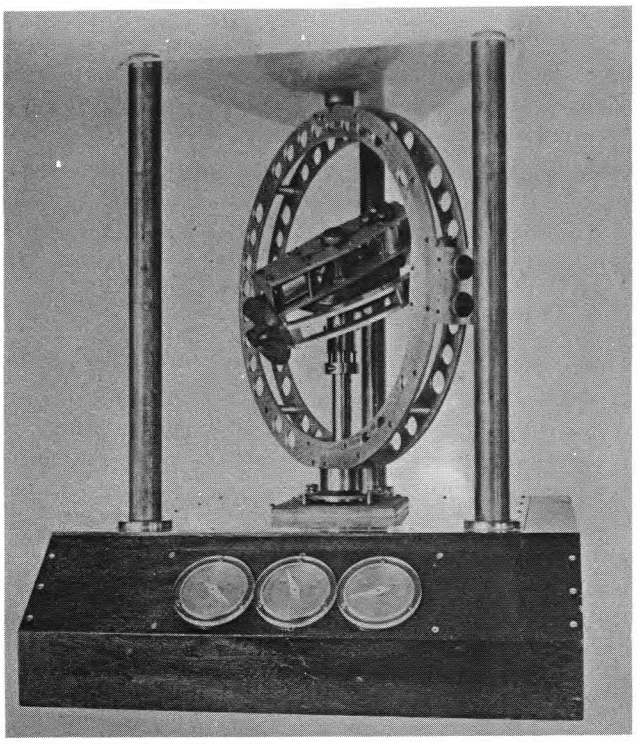

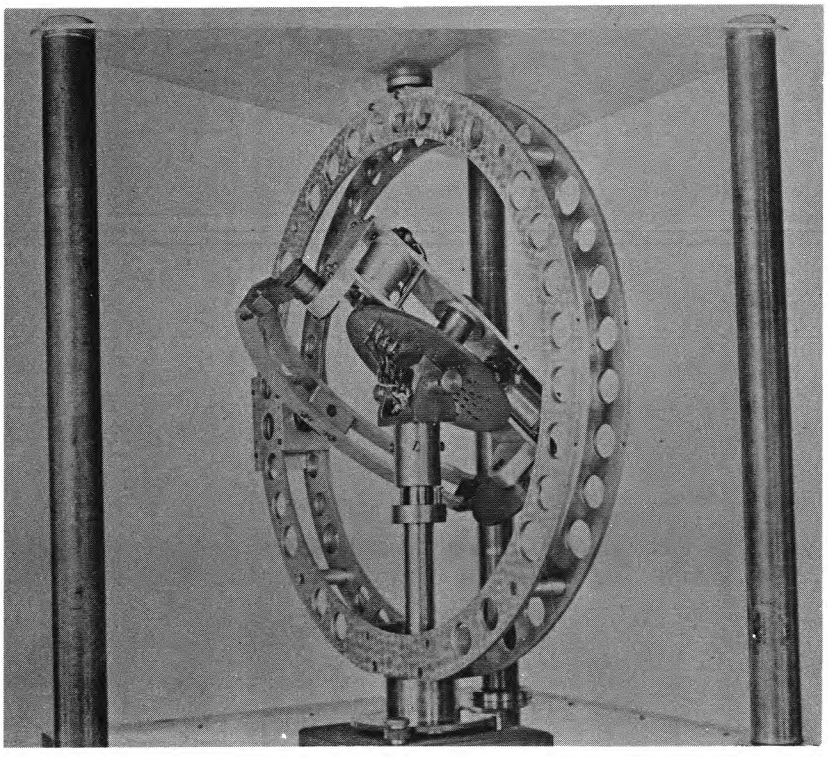

PLATE II - Views of Equatorial Drive.

References

1. Hey, J. S., Nature, 157, 47 (1946).
2. Piddington, J. H., and Minnett, H. C., Aust. J.Sci.Res., A, 4,131 (1951).
3. Martyn, D. F., Nature, 159, 26 (1947).
4. Hagen, J. P., N.R.L. Report 3504 (1949).
5. Smerd, S. F., Aust. J. Sci.Res., A,3,34 (1950).
6. Stanier, H. M., Nature, 165, 354, (1950).
7. O'Brien, P. A., and Tandberg-Hanssen, E., Observatory, 75, 11 (1955).
8. Van de Hulst, H. C., Bull. Ast. Inst. Neth., 11, 135, 150 (1950).
9. O'Brien, P. A., Mon.Not.Roy.Astron.Soc., 113, 597 (1953).
10. Covington, A.E., and Broten, N. W., Astrophys.J., 119, 569 (1954).
11. Christiansen, W. N., Nature, 171, 831 (1953).
12. Swarup, G., and Parthasarathy, R., Observatory, 75, 8 (1955).
13. Christiansen, W. N., and Warburton, J. A., Observatory, 75, 9 (1955).
14. Denisse, J. F., Blum, E. J., and Steinberg, J. L., Nature, 170, 191 (1952
15. Hey, J. S., and Hughes, V. A., In preparation.
16. Piddington, J. H., Astrophys. J., 119, 531 (1954).
17. Covington, A. E., Nature, 159, 405 (1947).
18. Christiansen, W. N., Yabsley, D. E., and Mills, B. Y., Aust. J.Sci. Res., A, 2, 506 (1949).
19. Piddington, J. H., and Hindeman, J. V., Aust.J.Sci.Res., A,2,524 (1949).
20. Hagen, J. P., et al, U.S. Naval Res. Lab.Reprint (March 1948).
21. Covington, A.E., Proc. I.R.E., 36, 454 (1948).
22. Denisse, J. F., C.R. Acad. Sci., 228, 1571 (1949).
23. Ryle, M., and Vonberg, D. D., Proc. Roy. Soc., A, 193, 98 (1948).

24. Pawsey, J. L., and Yabsley, D. E., Aust. J. Sci.Res., A,2,198 (1949).

25. Lehany, F. J., and Yabsley, D. E., Aust. J. Sci.Res., A,2, 48 (1949).

26. Waldmeier, M., and Muller, H., Z. Astrophys., 27, 58 (1950).

27. Payne-Scott, R., and Little, A.G., Aust.J. Sci. Res., A,4,508 (1951).

28. Machin, K.E., and O'Brien, P.A., Phil. Mag., 45, 973 (1954).

29. Dodson, H.W., Hedeman, E., and Covington, A.E., Astrophys.J., 119, 541 (1954).

30. Wild, J. P., Aust. J. Sci. Res., A, 3, 399 (1950).

31. Wild, J. P., Murray, J.D., and Rowe, W.C., Nature, 172, 533 (1953).

32. Little, A.G., and Payne-Scott, R., Aust. J.Sci.Res., A,5, 328(1952).

33. Hey, J.S., Parsons, S.J., and Phillips, J.W., Mon. Not.Roy.Astron. Soc., 108, 354 (1948).

34. Dodson, H.W., Hedeman, E.R., and Owren, L., Astrophys.J., 118, 169 (1953).

35. Hey, J.S., and Hughes, V.A., Nature 173, 771 (1954).

36. Hey, J. S., and Hughes, V.A., Mon.Not.Roy.Astron.Soc., In Publication.

37. Dicke, R.H., M.I.T. Radiation Lab. Rep. No. 787 (1945)

38. Hughes, V.A., Unpublished M.O.S. work.

39. Hughes, V.A., and Treadwell, E.E., Unpublished M.O.S. Work.

THE NATURE OF THE RADIO EMISSION FROM THE GALAXY AND DISCRETE SOURCES

by R. L. Adgie, B.A.

Radio Astronomy has made enormous progress since Jansky's original discovery in 1932[1] of a radio frequency radiation with an origin beyond the earth, but the process by which these waves are generated is still not fully understood. It is the object of this article to review the experimental evidence at present available and to outline briefly some of the possible radiation mechanisms.

The General Background Radiation

There are two parameters of the background radiation which can be determined at a given frequency - the spatial distribution and the absolute intensity. All the results at various frequencies show the same general features in spatial distribution, i.e., the "contours of radio brightness" follow roughly the distribution of visual stars throughout the galaxy with a maximum towards the galactic centre.[2,3,4] But the integrated radiation from the stars, radiating with the same intensity as the sun, is too small to account for this general background. Apart from a spectral line of hydrogen at 1420 Mc/s, the power per unit bandwidth varies only slowly with frequency. In this respect the spectrum of the emission is similar to the continuous or white light spectrum of sunlight, and in fact the emission is described by some radio engineers as "white noise".

The signal fed to the receiver has of course an amplitude which is fluctuating in a random manner, but the noise power in a given bandwidth can be defined as the R.M.S. value averaged over a sufficiently long period. This type of signal is also produced by the receiver itself and one of the technical problems of Radio Astronomy is to measure the noise signals picked up by the aerial in the presence of this receiver noise.

The normal method of designating the brightness of the background radiation is in terms of the flux radiated by unit area into unit solid angle. Figure 1 shows the spectrum of the background radiation plotted in these units and also two curves for black body radiators at temperatures of 1000 degrees and 10,000 degrees. The spectrum of the background does not coincide with any black body curve but it is frequently convenient to express the brightness at one frequency in terms of the temperature of a black body that would have the same brightness at that frequency. The apparent temperature of the background therefore rises rapidly at low frequencies.

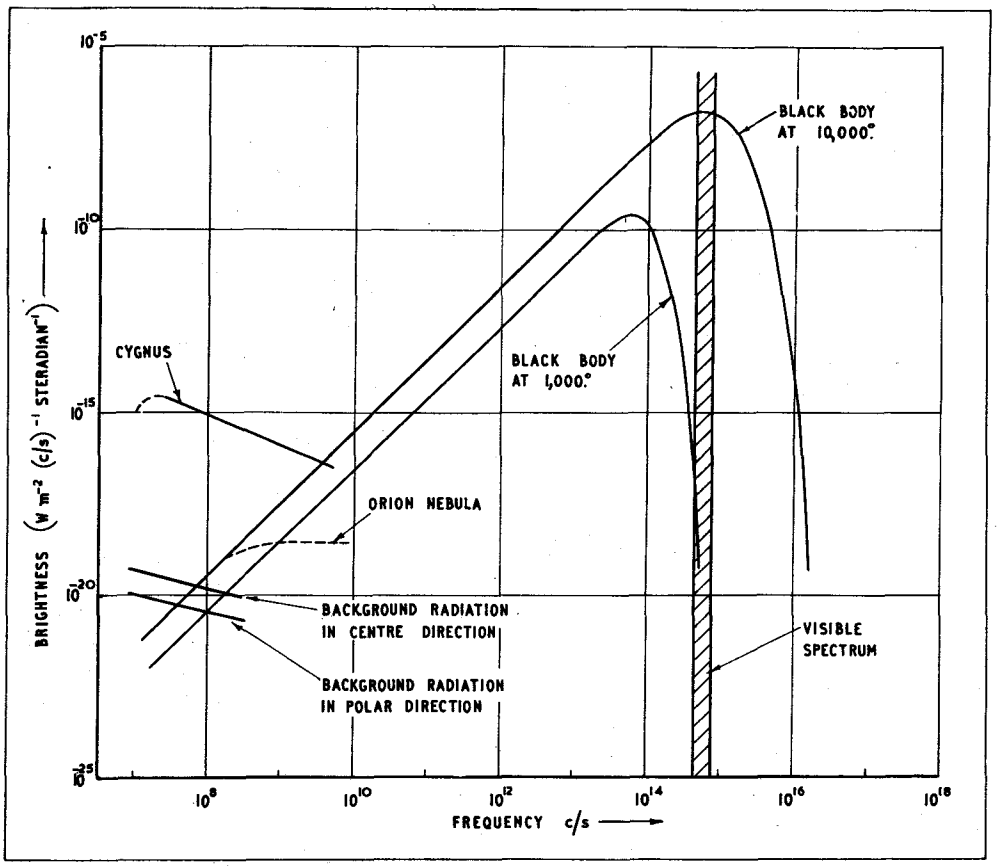

Figure 1

Variation of Brightness with Frequency

The full expression for the black body curve is given by Planck's theory:-

$$B = \frac{2h\nu}{e^{h\nu/kT}-1} \frac{\nu^2}{c^2} d\nu$$

where B is the brightness, T the temperature, h Planck's constant and k Boltzmann's constant.

When $h\nu$ is small compared to kT (corresponding to classical physics), the formula approximates to

$$B = \frac{2kT\nu^2}{c^2} d\nu$$

which is the Rayleigh-Jeans Law.

As can be seen from the black body curves in Figure 1, the Rayleigh-Jeans Law will be applicable at radio frequencies. (On the log scales used, $B \propto \nu^2$ corresponds to a straight line of slope 2).

In m.k.s. units the Rayleigh-Jeans Law gives

$$B = 3.06\ 10^{-40}\ T\nu^2\ (W\ m^{-2}\ (c/s)^{-1}\ steradian^{-1}\ *$$

The observed background temperature at 9 Mc/s is greater than 1000,000 degrees[5], which suggests a very efficient radiating mechanism that gives a brightness far greater than the expected thermal radiation**.

All the background surveys show a surprisingly large intensity in the direction of the galactic poles, far more than would be expected from an interstellar origin. This was thought to be the unresolved radiation from many extragalactic radio sources, but two pieces of information obtained at Cambridge have indicated a new possibility[6,7].

The Andromeda Nebula is a nearby galaxy and, like our own galaxy, produces non-thermal radio emission. But more than half of the total radiation appears to originate from regions having a spherical distribution extending well outside the galactic

---

* The steradian is the unit of solid angle.

** Interstellar gas has a temperature of about 100 degrees which rises to about 10,000 degrees close to hot stars.

plane. This spherical distribution also fits the contours of brightness found in our own galaxy and accounts for most of the radiation observed at the galactic poles. Figure 2 illustrates this "radio galaxy". The discovery of this new distribution does of course raise the difficulty of finding an explanation for its origin, as very few visual stars are observed at such large distances from the galactic plane.

The background has the same radio spectrum for different directions[8] and it seems natural to suppose that both the galactic and spherical distributions originate from similar emission mechanisms. At 81.5 Mc/s the background temperature near the galactic poles is about 1000 degrees[7]; the brightness varies as $\nu^{-0.5}$ [8] giving a variation of apparent temperature of $\nu^{-2.5}$. Therefore at the lower frequencies, the whole of the sky appears, to an aerial, to be very hot and the radiation that is received will normally produce more noise than the receiver itself.

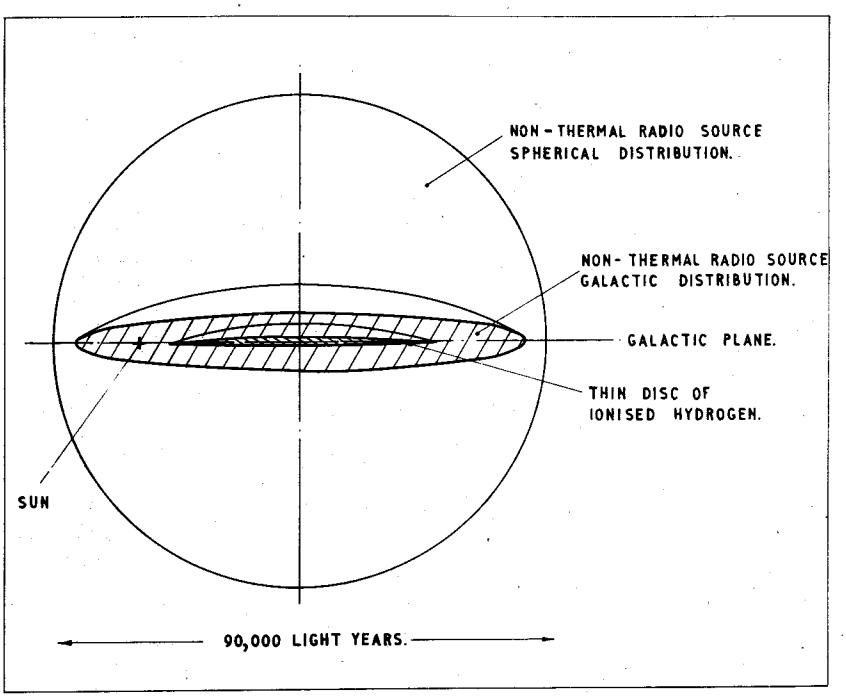

Figure 2

A Section through the "Radio Galaxy"

Galactic Thermal Emission from Ionised Hydrogen

Close to bright stars, clouds of hydrogen become ionised by the intense radiation and, having a kinetic temperature of about 10,000 degrees, can produce sufficient thermal radio emission to be detected.

In the rarefied ionised gas (the density is about 1 atom per c.c.) the electrons will be accelerated into hyperbolic orbits as they approach near to a proton and generate electromagnetic radiation. The loss of energy by the electron is not limited to specific values, as in transitions between fixed atomic energy levels, and the radiation will have a continuous spectrum with an intensity appropriate to the electron velocities. The electron velocities will be determined by the thermal agitation of the gas and the intensity of the radiation will correspond to the actual gas temperature. (A similar process produces the continuous X-ray spectrum, except that in this case the electrons are not thermal but have been accelerated to high velocities by the anode-cathode potential).

The full black body brightness will not be produced if the ionised gas cloud is semi-transparent. If the absorption coefficient is x, then the brightness will be:-

$$B = B_0 \left(1 - e^{-\int x ds}\right)$$

where B_0 is the black body brightness.

$\int x ds$ is the integral of the absorption along a line of sight through the cloud, and is called the "optical depth". For large values of optical depth, B approaches B_0, but for small values, $B = B_0 \int x ds$. Now x varies as ν^{-2} and B_0 as ν^2 so B becomes independent of ν when the cloud is "optically thin".

The large ionised gas cloud known as the Orion Nebula was first detected at 3000 Mc/s[9] with an apparent temperature of 100 degrees, i.e., $\int x ds = 0.01$, so the cloud is "optically thin" at this frequency. The brightness curve is shown in Figure 1; as the cloud becomes optically thick at low frequencies it joins the 10,000 degree black body curve and its brightness then rapidly falls until it equals that of the background at about 50 Mc/s. Below this frequency the cloud would be detected as a cold area in the hot background.

In addition to several isolated ionised clouds, a continuous band has been detected which is confined to the galactic plane[10] due to a thin disc like concentration of bright stars. Figure 3 shows the

appearance of this narrow band when seen both in emission and absorption the transition from optically thin to optically thick occurring at about 50 Mc/s. At frequencies above about 500 Mc/s the non-thermal background falls below the detection limit of most receivers, but the ionised hydrogen still remains sufficiently intense to be detected.

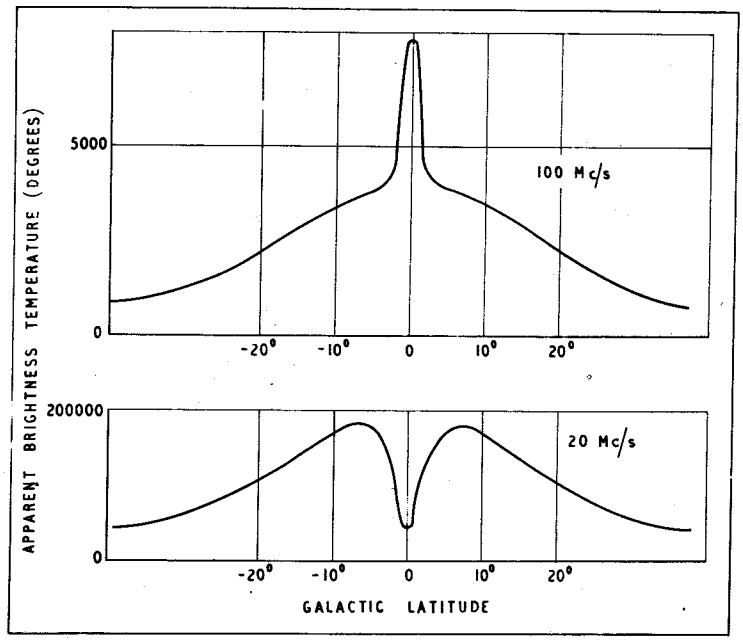

Figure 3

The Effect of Ionised Hydrogen on the General Background Radiation

The diagrams show the approximate variation of brightness temperature that would be obtained if a narrow beam aerial were swept across the galactic plane close to the galactic centre.

Discrete Sources of Radio Emission

A search for discrete sources has recently been completed at Cambridge,[11] giving a total of 1936 sources. 30 of these have large angular diameters between 20 min. and 2° of arc, and appear to be concentrated in the galactic plane. The remainder have small angular diameters and appear to be isotropic.

Knowing the intensity and angular diameter, the brightness can be computed; as with the background radiation, it is far in excess of that expected from a thermal emission mechanism.

The approximate brightness curve for the intense radio source in Cygnus is shown in Figure 1; the apparent brightness temperature rises to about 10^{10} degrees at low frequencies*.

A few of the most intense sources have been observed over a wide range of frequencies and they all appear to have spectra similar to that of Cygnus.

The brightness variations range from $\nu^{0.0}$ to $\nu^{-1.2}$ with an average of $\nu^{-0.6}$ [8]. This average is close to the value observed for the general background radiation. But the integrated radiation from many discrete sources of the type already observed falls well short of the observed background brightness, and to account for the increase of brightness in the galactic plane a far larger degree of galactic concentration would be required.

It is possible that the background is the integrated radiation from a different class of discrete sources whose brightness is too low to allow them to be observed individually, but having a very high density.

About 20 of the discrete radio sources have been identified with visual objects and a comparison of the optical and radio data provides valuable information about radiating mechanisms.

Identified Galactic Objects

The remnants of the two supernovae of 1054 (Crab Nebula) and 1604 (Kepler's Supernova) form powerful radio sources but appear as fairly faint visual nebulosities.

---

* There is now some evidence that the brightness begins to fall again below 20 Mc/s[12].

Several other faint nebulosities are associated with radio sources (including the most intense source in Cassiopeia) but their origin is unknown.

The optical measurements show violent internal motions in these sources, indicating severe turbulence. This mechanical energy of motion must, by some means, be translated into intense radio emission.

The extensive dust clouds prevent any visual observations in many directions in the galactic plane without affecting the transmission of radio waves. Several of the large diameter sources observed close to the galactic plane must be galactic objects, but their identification with visual objects will be prevented by this dust.

Identified Extragalactic Objects

The radio emission from about 10 galaxies has been detected,[13] including the Andromeda Nebula, and their brightness agrees roughly with the brightness of our own galaxy, i.e., they are normal non-thermal emitters.

The other radio sources identified as galaxies have all shown an extremely high radio brightness which is associated with some peculiarity in the galaxy. For example, the intense radio source in Virgo has been identified as NGC 4486, a galaxy having a very high velocity jet of material ejected from one side. Five of these "peculiar" objects have been identified as two galaxies very close together and probably in collision, the well known examples of this class being the intense source in Cygnus.

During the collision the stars in each galaxy, being separated by such enormous distances, will pass between each other unimpeded, but the interstellar gas will be subjected to large changing gravitational fields and will probably be set into violent turbulent motion. These conditions are similar to those existing, on a much smaller scale, in the galactic radio sources, and it is probable that the same mechanism produces the radio emission*.

As a result of the collision, the radio brightness of Cygnus has been increased by a factor of 10^5 over a normal galaxy, and it is interesting to speculate on the plight of an observer living in the centre of Cygnus. The visual effects of the collision would be very small, only an abnormal distribution of stars. At radio

---

* No significant differences in radio spectra have been observed for the galactic and extra-galactic sources.

frequencies the background radiation would be really intense, making it extremely difficult to detect the discrete sources of radio emission and producing very large noise powers in low frequency receivers. For example, at 50 Mc/s the equivalent brightness temperature would be about 10^9 degrees and the noise power produced at the input of a receiver would be about 10^6 times the receiver noise. (The noise voltage produced in a bandwidth of 4 Mc/s would be about 2 mV).

The Cygnus source is as much as 200 million light-years away and yet is the second most intense radio source. If it were at 10 times this distance it would be beyond the range of the 200 inch telescope at Mount Palomar but would still remain fairly intense at radio frequencies (the weakest sources obtained in the Cambridge survey are less than one thousandth of the intensity of Cygnus). It seems very likely that most of the weak radio sources found in the Cambridge survey are examples of colliding galaxies which are too distant to be observed with even the largest optical telescope(14).

Radio observations can therefore give valuable information about parts of the universe inaccessible to optical instruments. It is possible to "see" to distant parts of our own galaxy where optical observations are impossible because of dust obscuration, and to very great distances into space. In addition to the non-thermal emission mechanism providing a very efficient radio frequency generator, the spectrum plays an important part in increasing the range of radio observations.

All the distant galaxies appear to be travelling away from us with a velocity proportional to their distance and this motion produces a doppler shift in the radiation which effectively shifts the spectrum to lower frequencies. Referring again to Figure 1, the optical emission comes from stars in these galaxies having a temperature of about 10,000 degrees, i.e., the optical frequencies lie near the maximum of the black body curve. A doppler shift of the spectrum to lower frequencies produces a very sharp reduction in brightness compared to an equivalent shift of the Cygnus spectrum.

Non-Thermal Emission

An efficient transformation of mechanical energy into electromagnetic radiation is possible with some form of coherent oscillator. It is now thought that the enhanced radiation from the sun is caused by plasma oscillations in the ionised corona, but it is difficult to account for the continuous spectrum observed in galactic radiation by such a process.

Electrons, having a small mass, would need only small amounts of mechanical energy to raise them to the high velocities required for intense radiation. The problem is to find a process which will first produce high velocity electrons and then accelerate them to produce electro-magnetic radiation.

It is thought that weak magnetic fields, of the order of 10^{-4} gauss, exist in the interstellar gas clouds, maintained presumably by the turbulent motion of the ionisation, and these clouds have random velocities of a few km/sec. A fast electron will be deviated from a straight path during its passage through a cloud and some of the momentum of the cloud will be imparted to the electron. An electron will spend longer in a cloud which is moving in the same direction as itself than one moving against it, so the result of many encounters will be to speed up the electron. This process can be considered as an attempt on the part of the electrons to reach thermal equilibrium with the gas clouds through elastic collisions, and though the clouds have only small random velocities, because of their large relative mass, they can accelerate the electrons to high energies*.

The transverse acceleration imposed by the magnetic fields will produce electro-magnetic radiation and, because of the relativistic velocities, this radiation will be confined to a narrow cone along the direction of travel. Thus, a given electron will produce a short pulse of radiation as the line of sight coincides with its trajectory, as shown in Figure 4.

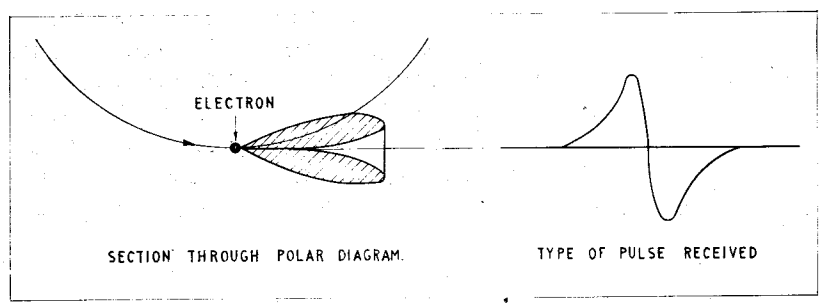

Figure 4

Radiation by Relativistic Electrons in a Magnetic Field

* Velocities are achieved which exceed 0.99995 c, corresponding to an energy of 100 times the rest mass. Energies of 10^5 times the rest mass are attained in some discrete sources.

The frequency spectrum will be given by the fourier components of this pulse and the frequencies having the largest amplitude will be close to[15]:-

$$\nu = 4.19\ 10^6\ B\ \gamma^2\ c/s$$

where B is strength of the magnetic field in gauss and the electron energy is γ times the rest mass.

The power radiated = $1.58\ 10^{-15}\ B^2\ \gamma^2$ ergs/sec.

Thus a radio frequency power spectrum of $\nu^{-0.5}$ should be associated with an electron energy spectrum of γ^{-2} *. The observed energy spectrum of cosmic rays is nearer to γ^{-3} but, since the cosmic rays measured are mainly protons, this difference may not be significant.

As yet no conclusive evidence has been found that cosmic rays originate from beyond the solar system, but the high energies measured in air showers do indicate the necessity for an accelerating mechanism operating in the interstellar space similar to that which gives the high energy electrons required for the production of radio frequency radiation.

Most theoreticians are satisfied that the non-thermal galactic radio emission is caused by relativistic electrons moving in magnetic fields, but the process which accelerates these electrons to high energies is not fully understood. The theory described above gives one possible solution to this problem, but unfortunately only operates on electrons with high initial energies. The turbulent motions associated with the discrete sources would certainly help to establish high energy gas clouds and their associated magnetic fields required by this theory. The initial high energy electrons could be produced by supernovae explosions or a thermonuclear reaction in colliding gas clouds.

References

1. Jansky, K., Proc. I.R.E., 20, 1920 (1932).

2. Hey, J. S., Phillips, J. W., and Parsons, S. J., Proc. Roy. Soc., 192, 425 (1948).

3. Bolton, J. G., and Westfold, K. C., Aust. J. Sci. Res., A, 3, 19 (1950).

---

* Radio frequency power in range ν to $\nu + d\nu$ is proportional to $\nu^{-0.5} d\nu$ which is therefore proportional to $(\gamma^2)^{-0.5}\ \gamma d\gamma$ or $d\gamma$

∴ No. of electrons in range γ to $\gamma + d\gamma$ is proportional to $\gamma^{-2}\ d\gamma$

4. Allen, C.W., and Gum, C.S., Aust. J. Sci. Res., A3, 224 (1950).

5. Higgins, C.S., and Shain, C.A., Aust. J. Phys., 7, 460 (1954).

6. Baldwin, J.E., Nature, 174, 320 (1954).

7. Baldwin, J.E., Reported at I.A.U. 1955.*

8. Adgie, R.L., Reported at I.A.U. 1955.

9. Haddock, F.T., Mayer, C.H., and Sloanaker, R.M., Astrophys. J, 119, 456 (1954).

10. Scheuer, P.A.G., and Ryle, M., Mon. Not. Roy. Astron. Soc., 113, 3 (1953).

11. Shakeshaft, J.R., et al., In publication and reported at I.A.U. 1955.

12. Lamden, R.J., and Lovell, A.C.B., Reported at I.A.U. 1955.

13. Pawsey, J.L., Reported at I.A.U. 1955.

14. Ryle, M., In publication and reported at I.A.U. 1955.

15. Hoyle, F., Nature, 173, 483 (1954).

---

* International Astronomical Union Symposium on Radio Astronomy, 1955.

BOOK REVIEW

THE THEORY AND PRACTICE OF COMMUNICATIONS, ELECTRONICS, FEEDBACK AND SERVOMECHANISMS
By J. Smith, 985 pp., 278 figs., Electron Press Ltd., London.

This book is of a very comprehensive nature, covering the theory and practice of communications, electronics, feedback and servomechanisms.

The author is to be congratulated on his choice of a heptode for the pre-amplifier in the non-linear multiple-loop guided weapon automatic launcher laying computer. A section describing the functions of the various grids would have been of value in this section, however.

There is an appalling error on p. 742 which spoils what otherwise might have been a fairly useful book. The author states that the conversion conductance of the 6L8G heptode usually lies between 0.35 mA/V and 0.40 mA/V. This is grossly misleading since it is only necessary to test a few dozen valves of this type to find one with a conversion conductance as low as 0.346 mA/V. Also, researches by the undersigned several years ago showed that it is possible to achieve a conversion conductance of 0.422 mA/V from this valve for short periods using three times the recommended heater voltage. Considerable space is devoted to the new cascode-hexode valve, the author succumbing to modern trends. Even though a conversion conductance of 19.7 mA/V up to 150 Mc/s is obtainable from this new device, there is still a lot to be said in favour of the well-tried heptode.

The author was formerly with a Government Research Establishment and he has restricted his scope to only those aspects of electricity which are investigated in these Establishments. This failing seems distressingly common nowadays, but nevertheless this book might prove a useful contribution. The book is printed on good quality paper and is handsomely bound in green leather with gilt embossed lettering.

P. PENTAGRID

(To would-be authors and reviewers - this may provide timely warning - Ed.)